Redox Control of Aluminum Ring-Opening Polymerization: A Combined Experimental and DFT Investigation

Junnian Wei, Madeline N. Riffel, and Paula L. Diaconescu*

Department of Chemistry and Biochemistry, University of California, Los Angeles, 607 Charles E. Young Drive East, Los Angeles, California 90095, United States

Supporting Information Placeholder

ABSTRACT: The synthesis, characterization, and reactivity of an aluminum alkoxide complex supported by a ferrocene-based ligand, (thiolfan*)Al(O^{t}Bu) (**1^{red}**, thiolfan* = 1,1'-di(2,4-di-*tert*-butyl-6-thiophenoxy)ferrocene), are reported. The homopolymers of *L*-lactide (LA), ε-caprolactone (CL), δ-valerolactone (VL), cyclohexene oxide (CHO), trimethylene carbonate (TMC), and their copolymers were obtained in a controlled manner by using redox reagents. Detailed DFT calculations and experimental studies were performed to investigate the mechanism. Mechanistic studies show that after the insertion of the first monomer, the coordination effect of the carbonyl group, which has usually been ignored in previous reports, can significantly change the energy barrier of the propagation steps, thus playing an important role in polymerization and copolymerization processes.

Introduction

The ring opening polymerization (ROP) of cyclic esters, epoxides, and carbonates has attracted much attention during the past few decades due to the impressive biomedical and pharmaceutical applications

of the respective polymers.[1-4] To date, a variety of ROP catalysts have been applied to the formation of homopolymers such as poly(lactide) (PLA), poly(ε-caprolactone) (PCL), poly(cyclohexene oxide) (PCHO), and poly(trimethylene carbonate) (PTMC).[1-13] However, a general method for synthesizing multiblock copolymers in one pot and/or with great control still remains a challenge.

Research in the area of ring opening polymerization has been focused mainly on the synthesis of new initiators/catalysts to increase reactivity and produce novel polymers.[6,7,14-17] Although the mechanisms of ROP, including cationic, anionic, coordination-insertion, activated monomer, and organocatalytic methodologies, are well-known and widely accepted, most of the computational mechanistic studies focus on homopolymers, and, specifically, only concern the first insertion step.[18-24] The propagation steps, which play an important role in stereocontrolled polymerization and synthesis of copolymers, are usually ignored.[25-27] As such, a better understanding of the mechanism is still essential.

In 2011, our group applied a redox switchable strategy to the ring-opening polymerization of different monomers by switching between the oxidized and reduced forms of a catalyst.[28] Since then, important progress in the area of switchable polymerization has been made by our group and others.[28-51] Via appropriate sequential catalyst oxidation and reduction, several types of di-block copolymers, such as PCL-PLA and PLA-PCHO, could be prepared. However, the substrate scope is still limited and the selectivity of the oxidized and reduced forms of the catalysts remains unclear.

Aluminum complexes are widely used in ring-opening polymerization.[52-56] Aluminum pre-catalysts with only one active alkoxide chain are facile to prepare, making it easy to control the polymerization and investigate the mechanism.[57-59] Thus, an aluminum alkoxide complex, (thiolfan*)Al(O^{t}Bu) (**1^{red}**, thiolfan* = 1,1'-di(2,4-di-*tert*-butyl-6-thiophenoxy)ferrocene), based on an OSSO ligand architecture,[40,60-72] was synthesized and studied in order to extend the redox-switchable ROP strategy to a broad substrate scope and to understand the mechanism. Herein, we report the polymerization of *L*-lactide (LA), ε-caprolactone (CL), δ-valerolactone (VL), cyclohexene oxide (CHO), and trimethylene carbonate (TMC, Chart 1) for

the formation of their respective homopolymers and copolymers. Detailed DFT calculations of the redox switchable strategy are reported that are also useful in understanding other coordination-insertion ROP processes, especially those focused on the formation of copolymers.

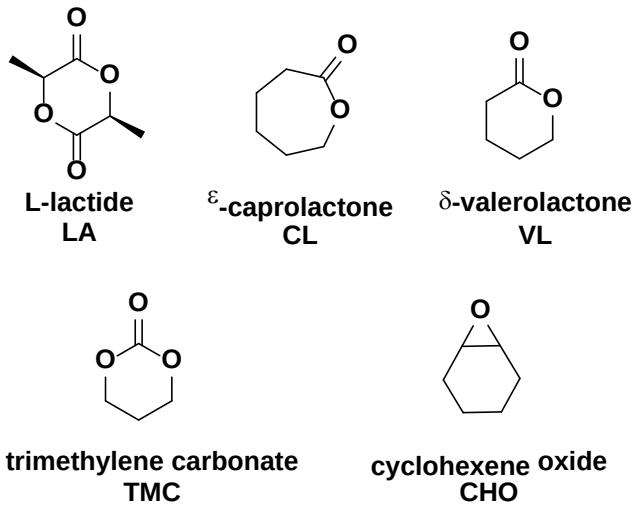

Chart 1. Monomers used in the present study.

Results and discussion

Synthesis and characterization of aluminum complexes. A successful synthesis of **1^{red}** is shown in Scheme 1. The reaction of $AlEt_2Cl$ and H_2(thiolfan*) in toluene at -78 ^oC led to the formation of (thiolfan*)AlCl (**1-Cl**), which then underwent a salt metathesis reaction with KO^{t}Bu, in a mixture of tetrahydrofuran (THF) and hexanes (Hex), to give **1^{red}**. It should be noted that other methods to prepare **1^{red}** failed, including the reaction of $AlMe_2(O^tBu)$ with H_2(thiolfan*).[73]

Compounds **1^{red}** and **1-Cl** are both yellow powders. Crystals of **1-Cl** suitable for X-ray diffraction could be obtained via recrystallization from toluene with a few drops of THF at -30 ^oC (Figure 1). The Al center is five-coordinated, similar to what was observed in other Al ROP pre-catalysts.[65,74-76] As there is one THF ligand present in the molecule, only one of the thiolfan* S atoms is coordinated to Al. Based on the structure of (thiolfan*)Ti(O^iPr)$_2$,[31] we propose that, in the absence of THF, both sulphur atoms are coordinated to Al. However, once a substrate (LA for instance) binds, one of them dissociates to keep the Al center

five-coordinated. This hypothesis is confirmed by our DFT calculations, which show two different Al-S distances when a monomer is coordinated to the Al center (for example, in the LA-**1**^{red} complex, the Al-S distances are 2.663 Å and 3.303 Å, respectively).

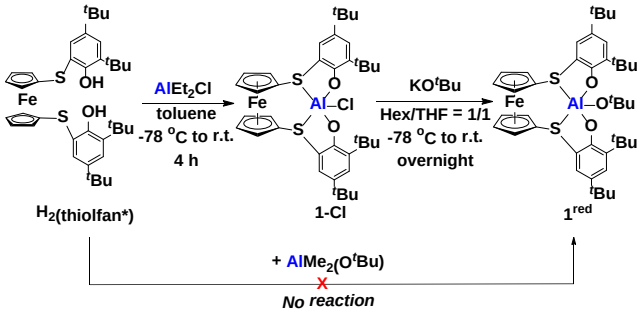

Scheme 1. Synthesis of **1**^{red}.

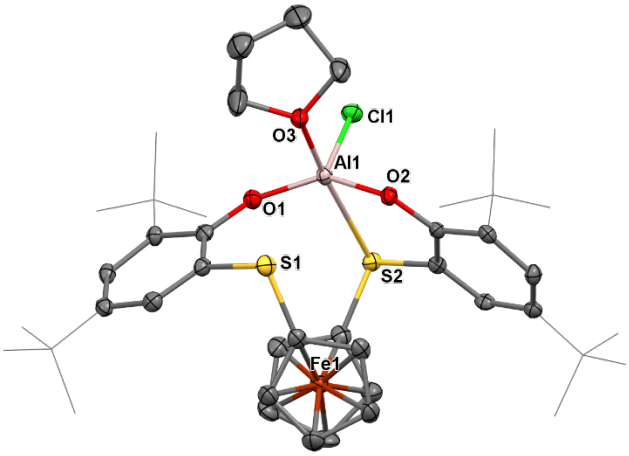

Figure 1. Molecular structure representation of **1-Cl**(THF) with probability ellipsoids shown at the 50% level. Hydrogen and solvent atoms were omitted for clarity. Selected distances (Å) and angles (º): Al1-O1 = 1.731(3), Al1-O2 = 1.741(3), Al1-S1 = 3.202, Al1-S2 = 2.727(2), Al1-Cl1 = 2.165(2); O1-Al-O2 = 143.62(16), O1-Al1-S2 = 89.88(12), O2-Al1-S2 = 79.03(11).

Electrochemical studies were performed with **1**^{red}. A quasireversible redox event (Figures S6-7) observed with $E_{1/2}$ = -0.023 V (vs $FeCp_2^{0/+}$) indicates that ferrocenium salts could oxidize **1**^{red}. Indeed, the addition of 1 equivalent of acetyl ferrocenium tetrakis(3,5-bis(trifluoromethyl)phenyl)borate ($^{Ac}FcBAr^{F}$)

in C_6D_6 resulted in the formation of a dark red product, [(thiolfan*)Al(O^{t}Bu)][BAr^F] (**1^{ox}**), within minutes. As expected, the corresponding ^{1}H NMR spectrum indicated the formation of a paramagnetic species. However, the ^{19}F NMR spectrum was more informative, showing a signal at -62.4 ppm that was assigned to **1^{ox}** as ^{Ac}FcBAr^F has poor solubility in C_6D_6. This paramagnetic product could be reduced back to the starting material **1^{red}** by the addition of an equivalent of $CoCp_2$. DFT calculations indicate that the singly occupied molecular orbital (SOMO) of **1^{ox}** is mainly localized on the ferrocene fragment (Figure 2). Thus, it should be possible to apply the redox-switchable strategy to compounds **1^{red}** and **1^{ox}** (Scheme 2).

Polymerization studies. Metal alkoxide species, M-OR, have been shown to be the true active species in numerous ROP processes.[1-13,18-24] For example, in 2004, Lewiński and co-workers reported the first structurally characterized aluminum ε-caprolactone complex, indicating that the Al-Me group has poor reactivity with CL.[77] Thus, in most ROP cases, an alcohol is used as an initiator and is essential in order to start the polymerization.

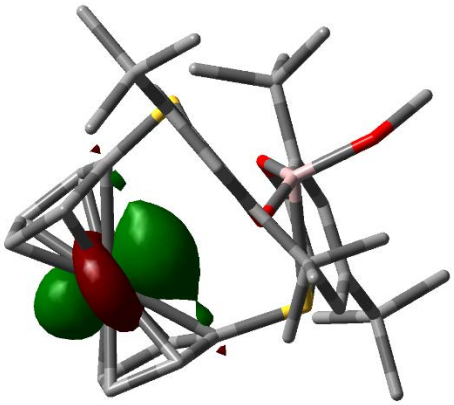

Figure 2. SOMO of **1^{ox}**.

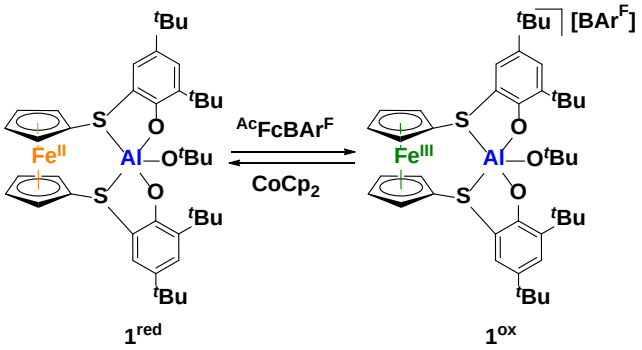

Scheme 2. Redox switching between $\mathbf{1}^{red}$ and $\mathbf{1}^{ox}$.

With $\mathbf{1}^{red}$ and $\mathbf{1}^{ox}$ in hand, the polymerization of various monomers was first tested (Table 1). The ROP of LA proceeded at 70 °C, while the ROP of other monomers was carried out at room temperature in C_6D_6. The polymers obtained from the above reactions were quenched by pouring the reaction mixtures into methanol and the precipitates were characterized by size exclusion chromatography (SEC, also abbreviated as GPC, gel permeation chromatography, in the text) with a multi-angle light scattering (MALS) detector.

In the polymerization of LA with $\mathbf{1}^{red}$, the molar mass corresponds well with the predicted value and has a narrow dispersity, while <5% conversion was observed with $\mathbf{1}^{ox}$ even at 100 °C overnight. These results were also observed with other redox switchable systems.[28,31,37,43,78]

However CL, VL, and TMC behaved rather differently (Table 1). Both forms, $\mathbf{1}^{red}$ and $\mathbf{1}^{ox}$, could polymerize these monomers, normally with lower rates for $\mathbf{1}^{ox}$ than $\mathbf{1}^{red}$. An explanation for this behavior is provided by DFT calculations and will be presented below. Herein, we discuss the experimental details of the ROP of CL as an example. In all cases, a higher molar mass than expected was observed. Although the polymer of CL obtained from a reaction carried out at room temperature has a relatively narrow dispersity (vs that obtained at 70 °C), its molar mass is much larger. These results could be attributed to a partial deactivation/inhibition of the catalyst, the occurrence of transesterification reactions (especially given the high temperature used), and/or to different initiation and propagation rates. An explanation for

the observed values will be discussed in the DFT calculation section. The ROP of VL and TMC behaved similarly (Table 1).

On the other hand, the activity toward CHO showed the opposite trend to that observed for LA: the conversion reached >90% within 20 min at room temperature with **1^{ox}**, while <5% conversion was achieved with **1^{red}** even at 70 ^{o}C overnight (Table 1).

The coordination-insertion mechanism is widely accepted in ROP systems with metal catalysts. An end-group analysis of our PLA by ^{1}H NMR spectroscopy (Figure S17) showed that the polymer was capped by an O^{t}Bu group, also indicating that this reaction proceeded through a coordination-insertion mechanism. Together with previous results from our group and others, we assume that the redox switchable catalysts with M-OR groups proceed through a coordination-insertion mechanism during a ROP process.

Table 1. Homopolymers prepared by **1^{red}** and **1^{ox}**.

							M_n[b]		
Entry	Catalyst	Monomer	Equiv.	Time (h)	T (^{o}C)	conversion[a] (%)	GPC[b]	Calcd.	PDI[c]
1	**1^{red}**	LA	100	24	70	88	1.1	1.3	1.08
2	**1^{ox}**	LA	100	24	100	<5	-	-	-
3	**1^{red}**	CL	100	6	rt	>95	4.0	1.1	1.30
4	**1^{red}**	CL	100	1	70	>95	1.5	1.1	1.61
5	**1^{red}**	CL	200	1	70	>95	6.4	2.3	1.10
6	**1^{ox}**	CL	100	72	rt	86	3.9	1.0	1.06
7	**1^{ox}**	CL	200	2	70	>95	6.2	2.3	1.09
8	**1^{red}**	VL	100	24	rt	69	4.7	0.7	1.31
9	**1^{ox}**	VL	100	24	rt	78	9.1	0.8	1.12

10	**1^{red}**	TMC	100	24	rt	95	3.9	1.0	1.54
11	**1^{ox}**	TMC	100	120	rt	74	4.9	0.7	1.43
12	**1^{red}**	CHO	100	24	70	<5	-	-	-
13	**1^{ox}**	CHO	200	0.3	rt	90	2.6	2.0	2.20

Notes. Reactions were carried out in NMR tubes and the conditions were not optimized. Catalyst (0.0025 mmol), C_6D_6 as the solvent (0.6 mL). Oxidant (^{Ac}FcBAr^{F}, 0.0025 mmol, 2.7 mg) was added to **1^{red}** to prepare **1^{ox}** *in situ*. LA = *L*-lactide, CL = ε-caprolactone, VL = δ-valerolactone, TMC = trimethylene carbonate, CHO = cyclohexene oxide. 1,3,5-trimethoxybenzene was used as an internal standard for the ROP of LA.

[a] Conversion calculated from *in situ* ^{1}H NMR spectroscopy by integration of polymer peaks versus internal standard or unreacted monomers.

[b] GPC measurements were performed in $CHCl_3$. M_n values are reported in 10^3 g/mol. Theoretical M_n values were calculated from conversion data. Measured dn/dc values: PLA, 0.026 mL/g; PCL, 0.062 mL/g; PVL, 0.029 mL/g; PTMC, 0.033 mL/g; PCHO, 0.082 mL/g.

[c] PDI = M_w/ M_n

In order to explain the above results, the propagation steps of ROP were considered. We first tested **1^{red}** in a reaction with only 2 equivalents of LA. As shown in Figure 3, the first equivalent of LA reacts with **1^{red}** within minutes at room temperature (for comparison, the polymerization of LA occurs at 70 ^{o}C). However, the other equivalent of LA remained unreacted even after 3 days at room temperature. Furthermore, the addition of 10 equivalents of CL at room temperature also led to no reaction (for comparison, the ROP of CL by itself is facile at room temperature), indicating that the propagation becomes difficult after the first insertion of LA.

In 2005, Lewiński and co-workers reported the crystal structure of an Al alkoxide complex obtained after the insertion of one equivalent of LA.[79] The newly formed Al complex, $[Me_2Al(\mu\text{-}OCH(Me)C(O))_2O(CH_2)_2OMe]_2$, containing a similar five-membered ring as **3**^{red} in Figure 3, was essentially inactive in the reaction with CL and LA unless heated at higher temperatures (70 ºC for example). Furthermore, in 2011, we reported a cationic yttrium complex, [(phosfen)Y(O^{t}Bu)][BAr^F] (phosfen = 1,1'-di(2-*tert*-butyl-6-diphenylphosphiniminophenoxy)ferrocene)), which could react with one equivalent of LA but could not react with another.[28] Those results indicate that the insertion of the first LA was facile in all those cases. However, after the first insertion, the strong chelation effect of the five-membered ring causes a significant rising in the activation barrier for the next insertion.

The fact that the activation barrier for the insertion of another LA increased indicates that the rate of the propagation step was much slower than that of the initiation step, guaranteeing living LA polymerization characteristics, with a narrow dispersity (Table 1). For other monomers (CL, VL, and TMC), the insertion of the first monomer would not cause such a significant chelation effect, implying a similar activation barrier for the propagation and initiation steps. This might cause broader dispersity values and higher molar masss (Table 1); such phenomena were reported in the literature without a detailed explanation.[80-85]

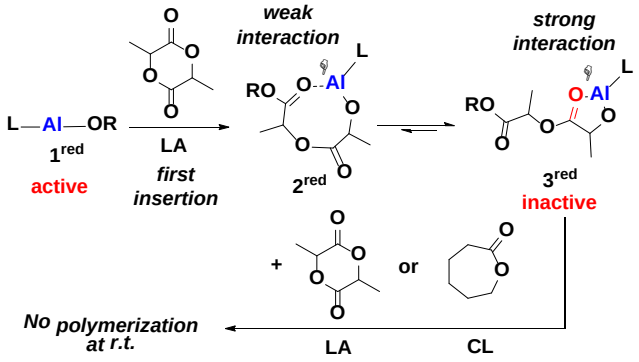

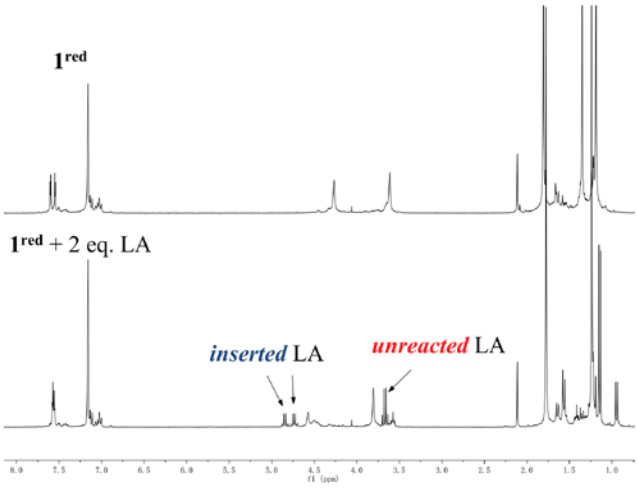

Figure 3. ^{1}H NMR (300 MHz, C_6D_6) spectra of the reaction between **1^{red}** and two equivalents of LA.

Previously reported examples of TMC polymerizations by aluminum complexes following a coordination-insertion mechanism also showed a broad dispersity together with higher than expected molar masss.[83-85] However, if the metal catalysts reacted as Lewis acids and TMC was polymerized by an appropriate Lewis acid/ROH pair instead, the PTMC material could be chain-length controlled.[53,85] These results indicate that mechanistic studies are important in order to design appropriate polymerization systems for different monomers.

Recently, Byers and co-workers reported that the polymerization of CHO, using a cationic iron(III) alkoxide complex, underwent a coordination-insertion mechanism and was non-living.[78] In the case of the CHO polymerization by **1^{ox}**, we also prefer a coordination-insertion mechanism rather than a cationic polymerization mechanism. This assumption is supported by DFT calculations (see the DFT calculation section). The polymerization of CHO by **1^{ox}** (Table 1) is also non-living because the barriers of the propagation and initiation are rather low and close in energy.

Kinetics studies of LA and TMC polymerizations were then carried out as examples. As shown in Figure 4, for LA, clear first-order kinetics were observed, as evidenced from the linear relationship between $\ln([LA]_0/[LA]_t)$ and time. Although the same first-order kinetics were observed for TMC with **1^{ox}**, a slow

initiation stage was present (nearly no polymerization occurred during the first 24 hours). For the ROP of TMC with **1**^{red}, a nonliving polymerization character was evidenced by the non-linear relationship between $\ln([TMC]_0/[TMC]_t)$ and time ($R^2 = 0.9226$), corresponding well with the above discussion.

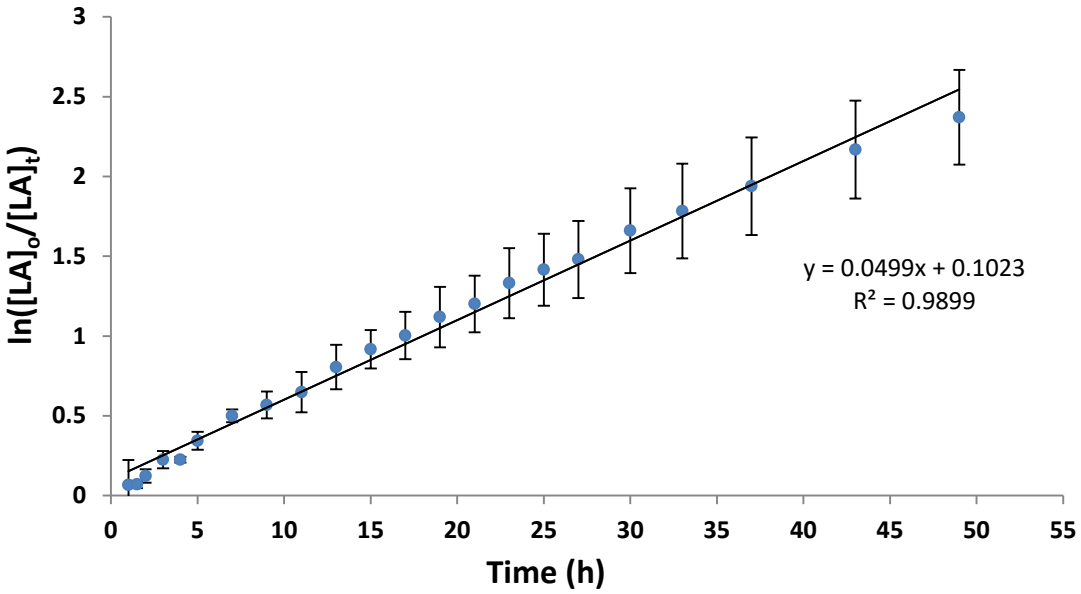

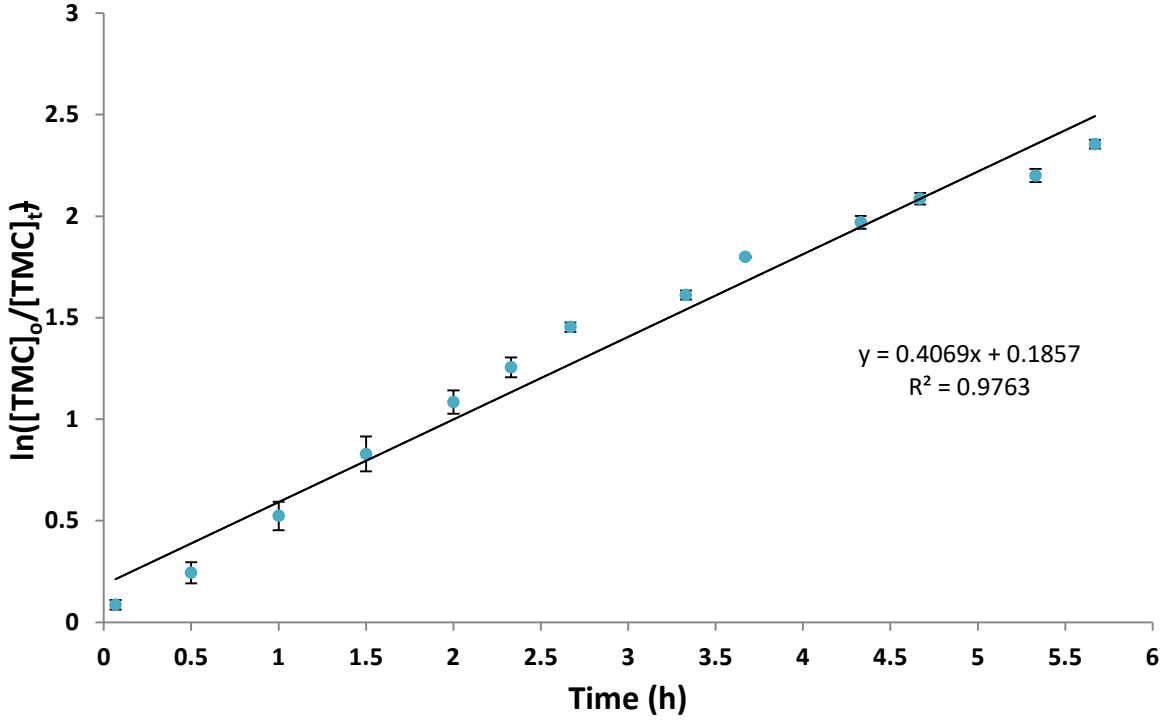
ln([TMC]o/[TMC]t)
Time (h)
y = 0.4069x + 0.1857
R² = 0.9763

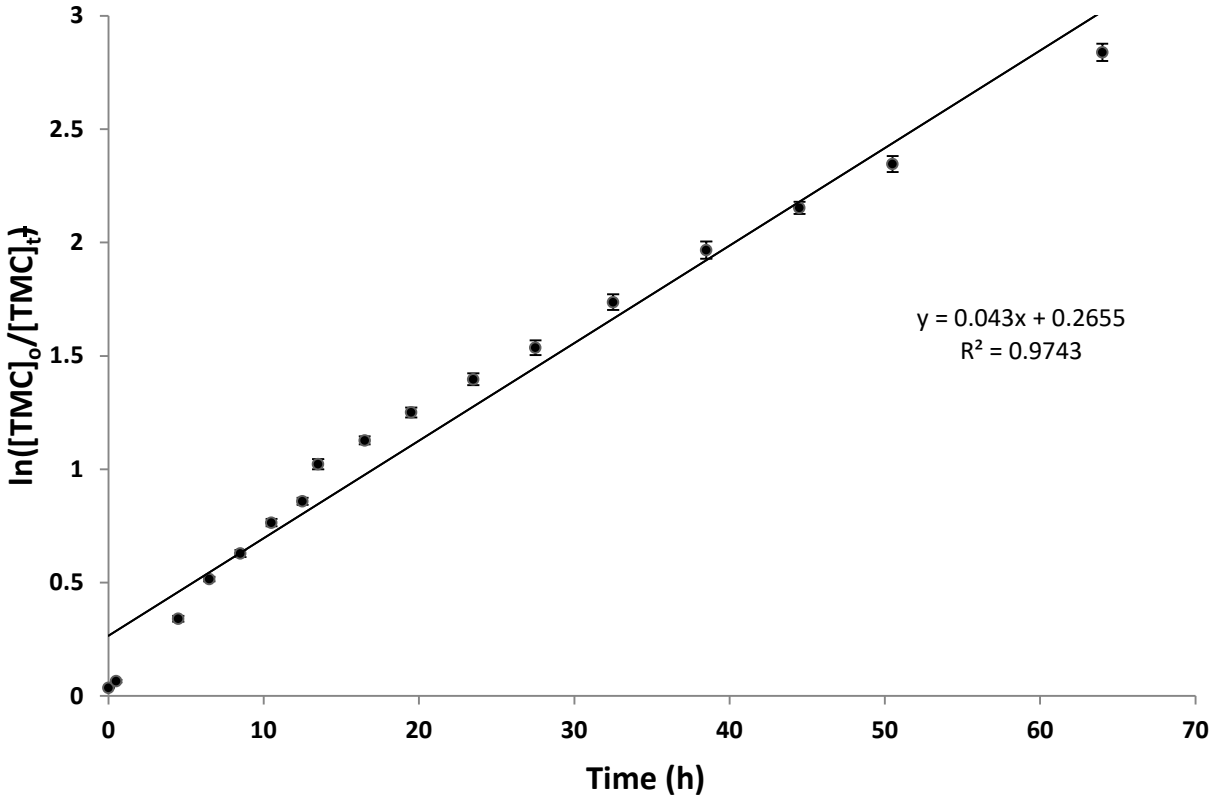
ln([TMC]o/[TMC]t)
Time (h)
y = 0.043x + 0.2655
R² = 0.9743

Figure 4. Kinetics studies of ROP of LA and TMC in C_6D_6: LA with $\mathbf{1^{red}}$ (top, standard deviation range: 0.0185 to 0.3078), TMC with $\mathbf{1^{red}}$ (middle, standard deviation range: 0.0043 to 0.0866), and TMC with $\mathbf{1^{ox}}$ (bottom, standard deviation range: 0.0024 to 0.0383). In all cases, [Monomer]/[Al] = 100, [Monomer] = 0.42 M. For each plot, three reactions were run and the average of the resulting data was obtained. The error bars are the standard deviation for the three samples. *Note*: Lactide was added as a solid due to its limited solubility in benzene. In this case, in order to obtain the initial lactide concentration, the integrations for the monomer and the polymer signals from the ^{1}H NMR spectra were added and averaged.

The copolymerization of two different monomers were tested next. As $\mathbf{1^{red}}$ and $\mathbf{1^{ox}}$ were both active for multiple monomers, making copolymers by either sequential addition or redox switchable polymerization of different monomers was possible. It would be beyond the scope of this article to explore all possible combinations. Herein, we only show the synthesis of several di-block copolymers as examples. It should be noted that it is theoretically possible to prepare multi-block polymers via this strategy.

The general procedures for preparing the copolymers are as follows. The first monomer (monomer A) is polymerized under the same conditions as those shown in Table 1. The second monomer (monomer B) is then added if making copolymers by sequential addition. When making copolymers by the redox switchable method, ^{Ac}FcBAr^F or $CoCp_2$ is added to change the oxidation state of the catalyst before adding monomer B. Polymer chain extensions are clearly demonstrated by comparing their GPC/SEC traces (increasing molar mass) with the corresponding polymers before adding monomer B (Figure 5 and Figures S1-5).

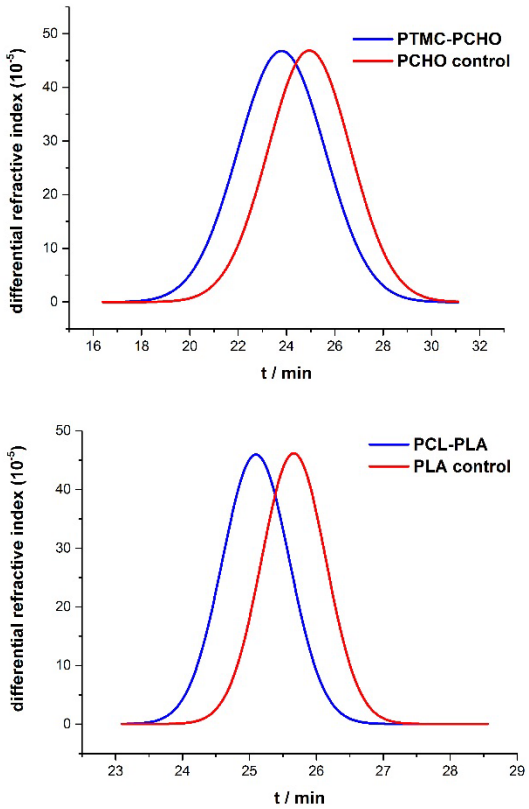

Figure 5. GPC/SEC traces of selected copolymers: Table 2, entry 3 (top) and Table 2, entry 7 (bottom). The blue lines correspond to copolymers and the red lines to the respective homopolymers before adding the second monomer. The baselines are calibrated, the peak area ratios are adjusted, and the curves are fitted by Gaussian distribution ($R^2 > 0.99$) to make them clear. The raw data can be found in the Supporting Information (Figures S35-52).

Because PLA-PCL di-block polymers prepared by sequential addition are widely studied and accepted,[5-8,10-13] we will discuss this system in detail later in the DFT calculation section as an example. Since **1**$^{\mathbf{red}}$ behaves similarly to other ROP Al catalysts,[5-13,52,53] herein, we will describe just the LA-TMC co-polymerization as an example. As shown in Table 2 (entry 1), we obtained a copolymer with a broad dispersity and higher molar mass than expected.

The oxidized catalysts usually have poor reactivity in other ROP systems.[28,39,40,43,44,49] Thus more examples studying sequential addition polymerization using **1**$^{\mathbf{ox}}$ were tested. The PCL-PCHO and PTMC-

PCHO di-block copolymers, which are relatively difficult to prepare by other methods, could be synthesized easily (Table 2, entry 2 and 3). The PLA-PCHO copolymer could not be made by simple sequential addition using **1^{ox}**, since LA itself could not be polymerized by **1^{ox}** (Table 1).

Several di-block copolymers could also be prepared by redox-switchable polymerization, such as PCL-PLA, PTMC-PLA, and PCHO-PCL (Table 2, entries 6 - 8), in addition to sequential addition (Table 2, entries 1-5). The PTMC-PCL copolymers (Table 2, entry 5) made by **1^{ox}** have a significantly higher molar mass (12.50 kDa) than expected (1.52 kDa) but show a narrow dispersity (1.03). This phenomenon is also observed in the homopolymers prepared by **1^{ox}**. We propose that the reason for these findings is that only a part of the catalyst is active during the polymerization. Detailed explanations will be given in the DFT calculation section.

Table 2. Data for selected copolymers prepared by **1^{red}** and **1^{ox}**.

Entry	Monomer A	Equiv.	Conv. (%)[a]	Redox reagent	Monomer B	Equiv.	t (h)	T (°C)	Conv. (%)[b]	M_n GPC[c]	M_n Calcd.	PDI[d]
1	LA/**1^{red}**	100	90	-	TMC	100	7	100	70	3.9	2.0	1.44
2	CHO/**1^{ox}**	200	>95	-	CL	200	72	rt	16	2.9	2.3	1.94
3	CHO/**1^{ox}**	200	>95	-	TMC	200	72	rt	50	4.4	3.0	1.54
4	CHO/**1^{ox}**	200	>95	-	LA	100	5	70	<5	-	-	-
5	CL[e]/**1^{ox}**	100	>95	-	TMC	100	48	rt	37	12.5	1.5	1.03
6	LA/**1^{red}**	100	83	^{Ac}FcBAr^{F}	CL/**1^{ox}**	50	18	70	26	1.5	1.3	1.11
7	LA/**1^{red}**	100	87	^{Ac}FcBAr^{F}	TMC/**1^{ox}**	100	18	70	12	1.7	1.4	1.12
8	CL/**1^{red}**	50	>95	^{Ac}FcBAr^{F}	CHO/**1^{ox}**	100	4	rt	>95	1.2	1.5	1.59

Notes. Conditions: monomer A was polymerized as mentioned in Table 1, C_6D_6 as the solvent (0.6 mL). ^{Ac}FcBAr^{F} or $CoCp^2$ was added to change **1^{red}**/**1^{ox}** *in situ*. LA = *L*-lactide, CL = ε-caprolactone, VL = δ-valerolactone, TMC = trimethylene carbonate, CHO = cyclohexene oxide. 1,3,5-trimethoxybenzene was used as an internal standard for the ROP of LA.

[a] Conversion calculated from *in situ* ^{1}H NMR spectroscopy by integration of polymer peaks vs internal standard or unreacted monomers.

[b] Conversion calculated from ^{1}H NMR spectra of isolated product by integrating the peaks of block B vs those of block A.

[c] GPC measurements were performed in $CHCl_3$. M_n values are reported in 10^3 g/mol. Theoretical M_n values were calculated from conversions. Measured dn/dc values: PLA, 0.026 mL/g; PCL, 0.062 mL/g; PVL, 0.029 mL/g; PTMC, 0.033 mL/g; PCHO, 0.082 mL/g.

[d] PDI = M_w/ M_n

[e] Reaction run in benzene.

DFT calculations. Computational studies have been increasingly used in the characterization of unknown chemical compounds, obtaining mechanistic information,[86-94] and predictive studies.[95-104] To gain a better understanding of the polymerization processes discussed above, detailed theoretical studies were essential. Our group previously reported DFT calculations on redox switchable polymerization by cerium.[43] Those calculation results showed that the activation barrier with the reduced form of the catalyst (5.9 kcal/mol) was lower than that with the oxidized species (10.5 kcal/mol) in the polymerization of LA. However, this data could not explain why the reaction would not take place with the oxidized catalyst at ambient temperature, as the barrier was relatively low. We propose herein that, for most redox switchable ROP processes, the initiation step is easy and fast in both catalyst states, while the rate of propagation varies from monomer to monomer, causing remarkable differences.

All calculations were carried out with the GAUSSIAN 09 program package[105] on the Extreme Science and Engineering Discovery Environment (XSEDE).[106] The O^{t}Bu groups were simplified to OMe groups and the methyl groups of LA were replaced by H atoms during the propagation steps. For the oxidized complex, [(thiolfan*)Al(O^{t}Bu)][BAr^F] (**1^{ox}**), which is an ionic compound with [BAr^F] as the counter anion,

the anionic part was ignored in order to simplify the calculations since it is not involved in polymerization directly. It should also be noted that using a dispersion correction is important and the D3 version of Grimme's dispersion[107] was applied. The polymerizations of LA, CL, TMC, and CHO were analyzed. As the mechanism of polymerization of CHO is quite different from that of the other monomers, we will first discuss LA, CL, and TMC together.

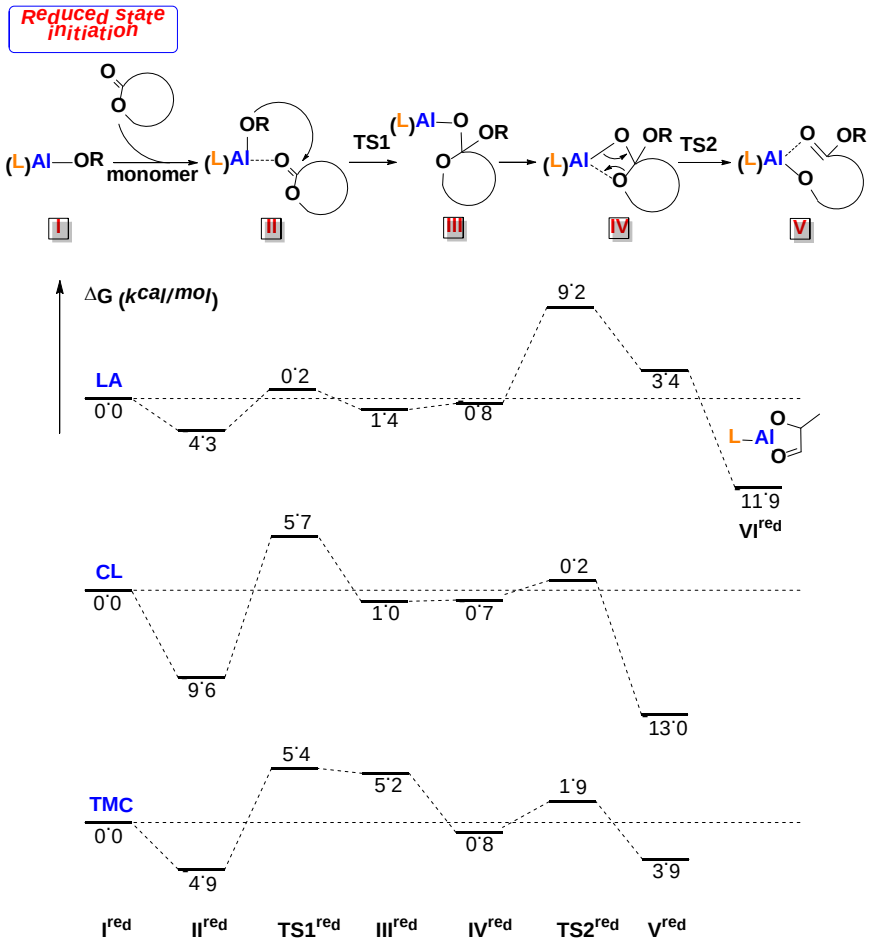

Figure 6. Potential energy surfaces of the initiation steps with $\mathbf{1}^{red}$.

Free energy surfaces of initiation and propagation steps with $\mathbf{1}^{red}$ and $\mathbf{1}^{ox}$ were performed. We first discuss LA as an example for the initiation step. The reaction of $\mathbf{1}^{red}$ begins with the coordination of LA to the Al center and the dissociation of one thiolfan* S atom. This coordination step is favored for all

monomers (Gibbs free energy ranging from -4.3 for LA to -9.6 kcal/mol for CL, Figure 6). Then, the first insertion of the coordinated LA occurs via a four-membered transition state with an energy barrier of only 4.5 kcal/mol. Although the energy barrier of the next step (ring opening) is higher (13.5 kcal/mol overall), the initiation step of LA with $\mathbf{1}^{red}$ is an easy process, which corresponds with the experimental results.

The initiation step of CL and TMC went through similar pathways with an activation barrier of 15.3 kcal/mol and 10.3 kcal/mol, respectively (Figure 6). Unlike for LA, for which the ring-opening step is higher in energy than the nucleophilic attack, for CL and TMC, the nucleophilic attack is the rate determining step (Figure 6).

Previous reports of ROP theoretical studies would assume at this point that the propagation step went through a similar pathway as the initiation step, with similar energy surfaces (path B in Scheme 3). Although this is a reasonable assumption in most cases, it is usually not true for LA. In addition, from our own experimental results, discussed above, and those of others,[1-13] the polymerization of CL usually goes faster than that of LA while making the corresponding homopolymers. However, when mixing LA and CL for the synthesis of copolymers, LA usually goes faster.[108-110] This phenomenon cannot be explained by accounting only for the energy barriers of the initiation step.

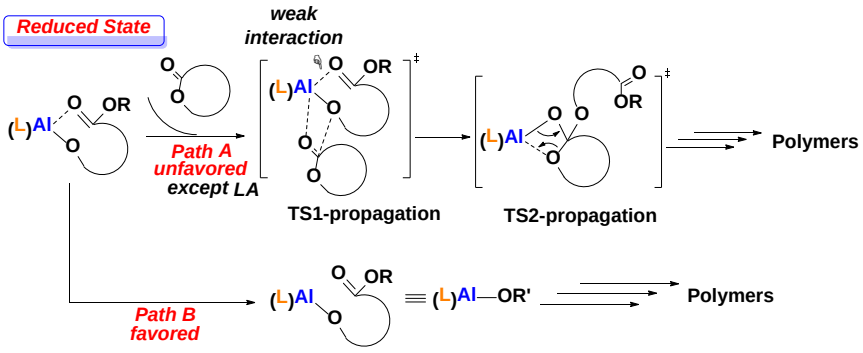

Scheme 3. General ROP propagation steps with $\mathbf{1}^{red}$.

The energy surfaces of the second insertion of CL or LA after the first insertion of LA were then performed (Figure 7). As the chelation of the first LA was strong, the five-membered ring remains intact during the second insertion, resulting in a higher energy barrier (20.1 kcal/mol for LA and 23.0 kcal/mol for CL) than for the initiation step. This finding is supported by a comparison of ^{13}C NMR spectra from the reaction of **1^{red}** with 1 and 5 equivalents of LA (Figure S26) that shows two types of carbonyl groups coordinated to the aluminum center.

After the insertion step (**TS1'**), the intermediate has a similar structure to that of the initiation step, so we estimated the energy barrier of TS2' in the propagation step by using the data from the initiation step as described in the following: after the initiation step, we forced the carbonyl group in **V** (Figure 6) to dissociate from the Al center (O-Al distance > 3 Å, **V-release**, not shown), optimized the structures and calculated the energy for **V-release**. It should be noted that **V-release** is not an actual intermediate for LA, however, it is an existing intermediate for CL, VL, and TMC. In the latter cases, after the first insertion, the C=O group will dissociate from the catalytic center to allow the second monomer to coordinate. Thus, it is important to consider **V-release** in order to obtain the correct energy barriers of the propagation steps. As **V-release** has a similar structure to the starting compound **I**, the same structures, **VII** and **TS2'**, would be obtained either from **VI** or **V-release** as the starting point. Therefore, by applying the energy difference between **V** and **V-release**, together with the data from the initiation steps, reasonable energies of **VII** and **TS2'** could be estimated (Table S2). The same strategy was also applied below for calculations involving the oxidized state catalyst (Table S2).

The insertion of the first LA is always facile (even more so than for CL), as the C=O group in LA is easily attacked by nucleophiles (-O^{t}Bu group). However, after the first insertion, the propagation becomes difficult for LA because of the formation of the five-membered ring intermediate (**3^{red}** in Figure 3, **VI^{red}** in Figure 6, both similar to $[Me_2Al(\mu\text{-}OCH(Me)C(O))_2O(CH_2)_2OMe]_2$ reported by Lewiński and coworkers),[79] which makes the coordination of the second LA to the catalytic center difficult. These results

provide good explanations for several important phenomena: 1) the temperature for the polymerization of LA (70 °C) is in agreement with a 20.1 kcal/mol energy barrier of propagation; 2) only one equivalent of LA undergoes insertion at room temperature (corresponding with a 13.5 kcal/mol energy barrier for initiation); 3) the homopolymerization rate of CL is faster than that of LA because the propagation of CL is faster than LA (no formation of the "five-membered ring"), however, when making LA/CL copolymers in one pot, LA is consumed first (once a LA inserted, the insertion of another LA is easier than that of CL, Figure 7) because LA is more electron deficient than CL.

On the other hand, based on previous reports,[5-13,18-27] after the insertion of the first equivalent of other monomers (CL, VL, and TMC), the rates of polymerization will not decrease remarkably, indicating that the insertion of the first monomers will not cause such a significant chelation effect like LA. Thus, in these cases, the energy of the initiation step can be used to estimate the energy of propagation.

However, as the reaction rates between initiation and propagation are close, the polymerization can be easily affected by the substituents of the ancillary ligand, the metal center, and the solvents. For example, in 2005, Darensbourg and co-workers reported the ROP of TMC by a series of Al and Sn salen (salen = *N*,*N*'-bis(salicylidene)ethylenediamine) complexes; for example, replacing the H in the phenolate rings with Cl would increase the TOF number from 46 to 81.[84]

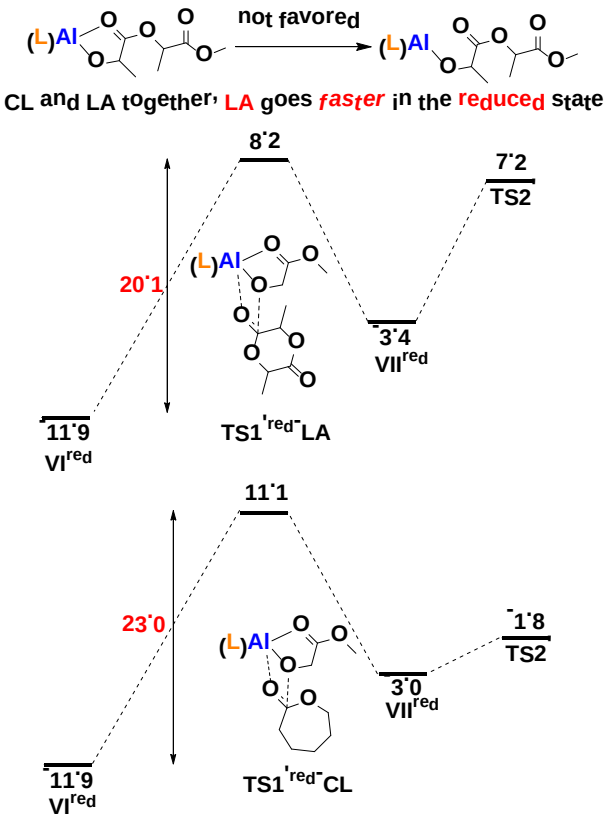

Figure 7. The potential energy surfaces of the propagation steps with $\mathbf{1}^{red}$ after the insertion of the first LA.

The polymerizations with $\mathbf{1}^{ox}$ were different. As the active species became a cation, the Al center was more electron deficient than in $\mathbf{1}^{red}$, resulting in a stronger interaction with the carbonyl group. As shown in Figure 8, the coordination of the monomers was also more favored (exergonic by 11.6 kcal/mol for LA to 19.3 kcal/mol for CL) than in the case of $\mathbf{1}^{red}$. The initiation steps with $\mathbf{1}^{ox}$ were quite similar to those with $\mathbf{1}^{red}$. It should be noted that the free energy surfaces are flat around the first transition state. The first transition states shown in Figure 8 of CL and TMC were located by approximation via scanning the energy surface. However, as the carbonyl groups from the monomers have strong interactions with the Al center, the first transition state (the nucleophilic attack) of the propagation steps was different from that of the initiation steps (Scheme 4). As shown in Figure 9, the activation barrier of the propagation process of LA

(24.3 kcal/mol) was higher than that of the initiation step (18.0 kcal/mol). Due to the strong chelation effect of the five-membered ring, no further insertion of LA would occur, resulting in no polymerization of LA with **1^{ox}**. Moreover, as shown in Figure 9, if we carried out the copolymerization of LA and CL in one pot with **1^{ox}**, only CL would be consumed.

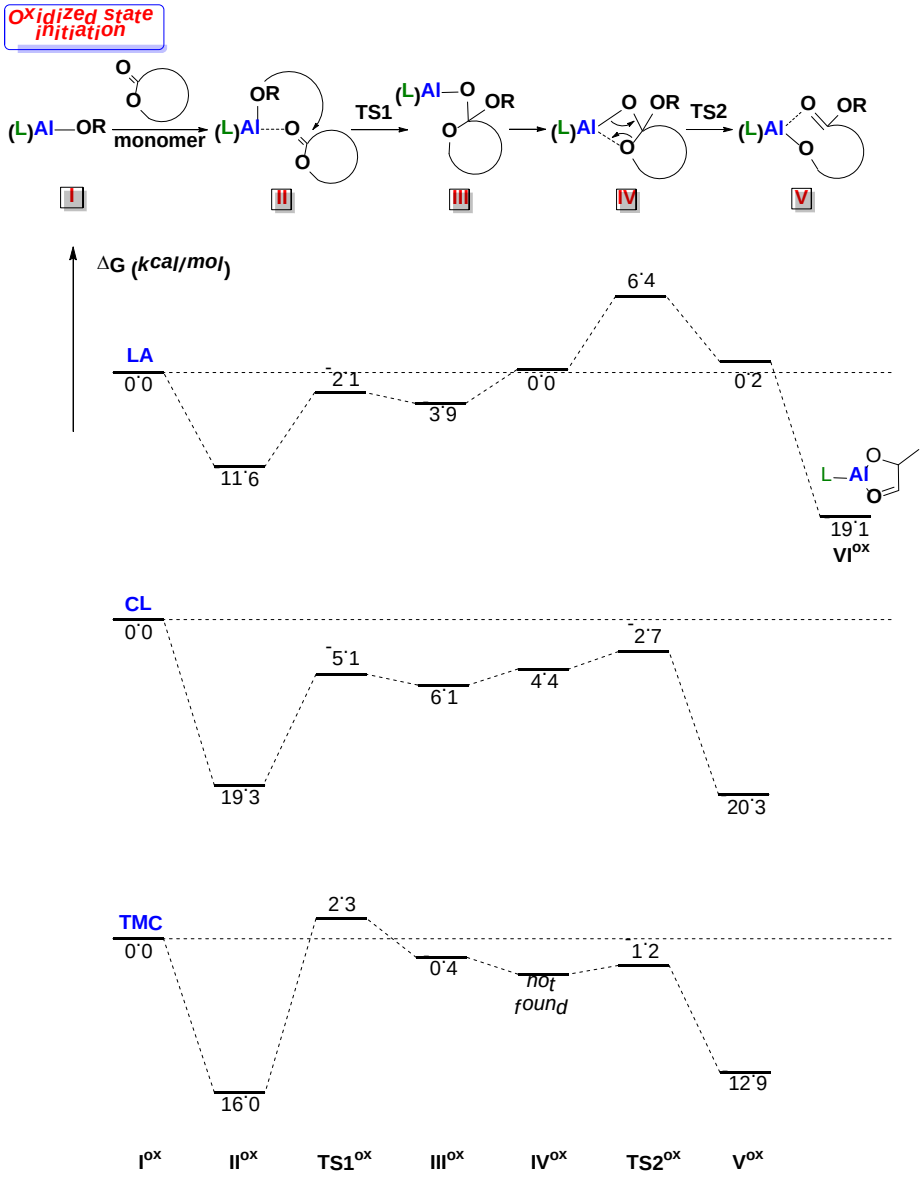

Figure 8. Potential energy surfaces of the initiation steps with **1^{ox}**.

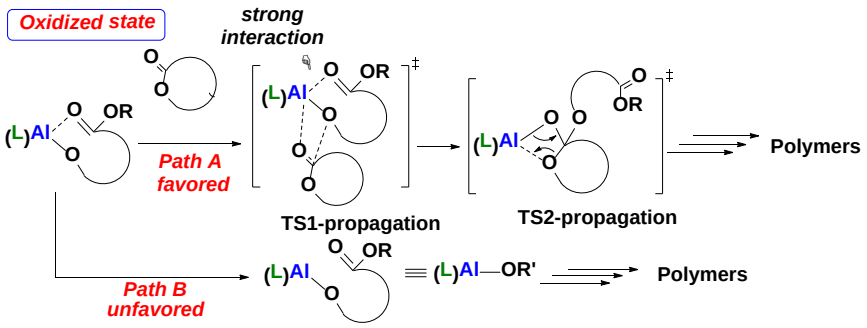

Scheme 4. General ROP propagation steps with $\mathbf{1^{ox}}$.

The polymerizations of CL and TMC are different from that of LA. As shown in Figure 10, the overall activation barriers of the propagation steps are lower than those of the initiation steps, meaning that the initiation would take a long time and thus lead to polymers with higher molar masss than expected. These results correspond well with our experimental results. Indeed, it takes days to consume the first 5% of TMC, while the rest is consumed much faster, producing high molar mass polymers.

It should be noted that the barriers from our DFT calculations with $\mathbf{1^{ox}}$ might be somewhat underesti-mated, as experimentally there was no polymerization of LA with $\mathbf{1^{ox}}$ even at 100 ^{o}C over 24 h, although the calculated barrier was 24.3 kcal/mol, meaning that the polymerization should occur at 100 ^{o}C in a reasonable time. This is likely a result of the simplifications we made, in particular, considering just the cationic part of $\mathbf{1^{ox}}$. However, the data is reasonable enough for us to understand the experimental trends and predict polymerization behaviors.

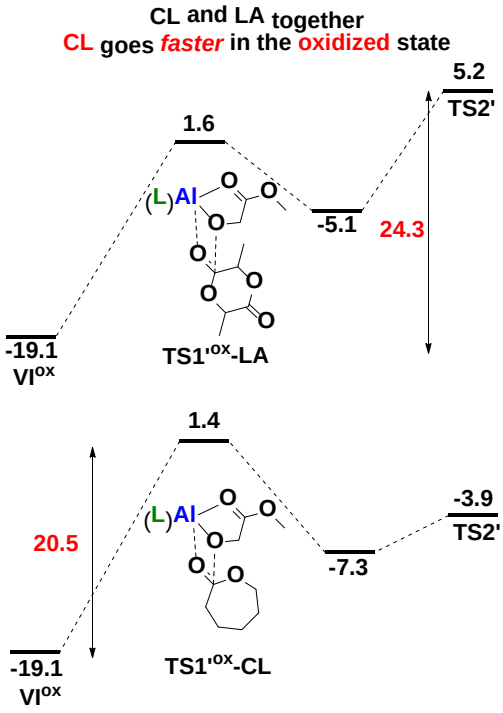

Figure 9. The potential energy surfaces of the propagation steps with **1**^{ox} after the insertion of the first LA.

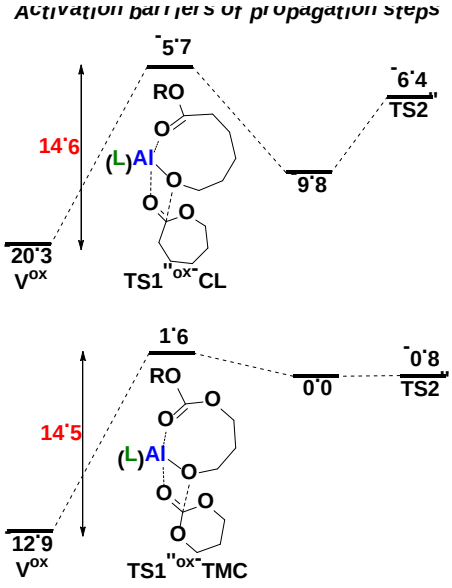

Figure 10. The potential energy surfaces of the propagation steps of CL and TMC with **1**^{ox}.

Natural bond orbital (NBO) analysis was also applied to understand the mechanism. The NBO charges of the Fe center are more positive in the oxidized than in the reduced state (Table 3), supporting the proposal that the redox reactions happen on the ferrocene fragments. The following discussion is focused on the interactions between the Al center and the carbonyl groups after the first insertion (stages **V** for CL and TMC and **VI** for LA). As shown in Table 3, the Al centers are more positive while the oxygen atoms from the carbonyl groups are more negative in the oxidized than in the reduced states. In fact, if considering the Wiberg bond order, which measures the extent of covalent interactions, the coordination effect of the carbonyl groups is stronger in the reduced than in the oxidized state. For example, after the insertion of the first CL, the Al-O_{CO} Wiberg bond order is 0.20 in the reduced state and only 0.06 in the oxidized state (for the Al-O_{CO} bond orders of other monomers, see Table S1). Thus, these results indicate that the interactions between the Al center and the carbonyl groups are mainly dominated by electrostatic effects for the oxidized systems.

Furthermore, the NBO charges of the alkoxide oxygen atoms were more negative after the insertion step than before for CL and TMC, while for LA, the oxygen atoms were more positive after insertion for both the reduced and oxidized systems. As the first step of ROP is the nucleophilic attack, the less negative the oxygen atom of the alkoxide group is, the more difficult the nucleophilic attack would be. Thus, these results partly explain why the propagation of LA is slower than initiation, while the propagations of CL and TMC are faster.

Table 3. NBO charge distribution.

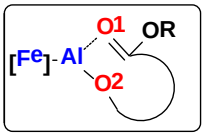

	Al	Fe	O1	O2

1^{red}	1.90	-0.22	-	-1.00
1-LA^{red}	1.97	-0.22	-0.68	-0.97
1-CL^{red}	2.01	-0.22	-0.71	-1.04
1-TMC^{red}	2.00	-0.21	-0.74	-1.05
1^{ox}	1.96	0.24	-	-1.01
1-LA^{ox}	2.03	0.24	-0.72	-0.98
1-CL^{ox}	2.08	0.22	-0.76	-1.05
1-TMC^{ox}	2.06	0.23	-0.78	-1.04

Combining these results, we could design a redox-switchable polymerization of LA and CL in one pot (Scheme 5). Although **1^{red}** can polymerize both LA and CL, LA would be consumed first while almost no conversion of CL would be observed during that time. This phenomenon was confirmed by ^{1}H NMR spectroscopy (Figure S34). After the addition of the oxidant, CL could then be polymerized while the polymerization of LA stopped (Figure S34). These observations are consistent with the experimental results.

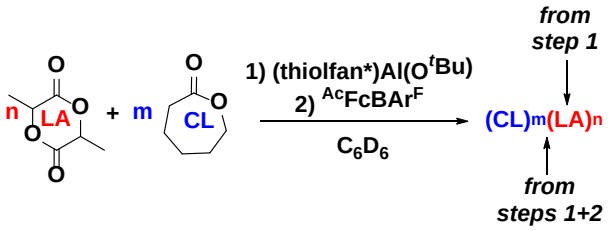

Scheme 5. One-pot synthesis of PLA-PCL copolymers by *in situ* switching.

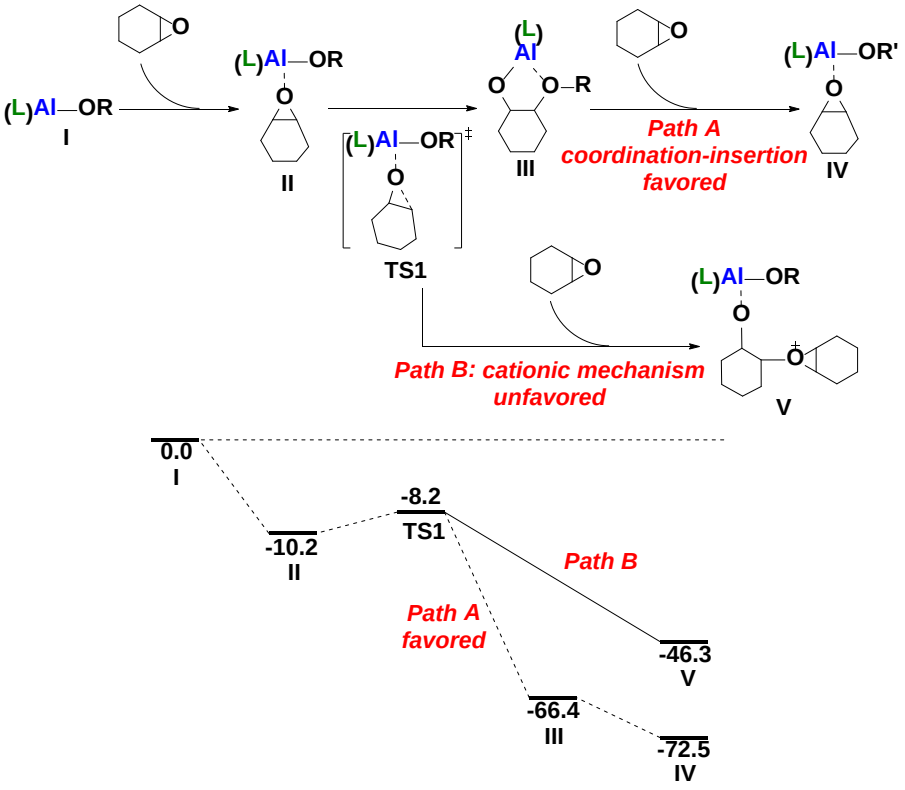

Figure 11. Potential energy surfaces of the ROP of CHO with **1^{ox}**.

DFT calculations for CHO were also performed. As shown in Figure 11, after the coordination of one CHO to the Al center of **1^{ox}**, the cleavage of the C-O bond in the three-membered ring was facile (with only a 2.0 kcal/mol energy barrier). Because of the presence of the alkoxide group on the Al atom, the formation of the five-membered ring intermediate **III** (path A) was favored over a cationic mechanism (path B).

Both the initiation and propagation activation barriers of CHO polymerization are around 2 kcal/mol. Although the barriers might be underestimated, they suggest a fast polymerization. Indeed, the polymerization of 200 equivalents of CHO in a J-Young NMR tube would finish within 20 min at ambient temperature. This could explain the broad dispersity values and the non-living character of the CHO polymerization.

After the polymerization of CHO, the PCHO chain is still connected to the Al center and can be regarded as an alkoxide group. Thus, the block copolymers PCL-PCHO and PTMC-PCHO could be prepared by the sequential addition of CL or TMC after the polymerization of CHO, while the PLA-PCHO copolymer could not be made via this method (Table 2), as the propagation of CL and TMC with **1^{ox}** was facile while with LA was not. Furthermore, since we can also polymerize CHO after the polymerization of CL (Table 2), this fact supports the proposal that the polymerization of CHO did not go through a cationic mechanism. Because the active center is not at the metal during a cationic polymerization, if the polymerization of CHO went through a cationic mechanism, we would get a mixture of the homopolymers PCL and PCHO instead of block copolymers, because aluminum has only one initiating alkoxide group and cannot tolerate a coordination number higher than five.

Conclusions

We synthesized and characterized a novel aluminum complex, (thiolfan*)Al(O^{t}Bu), and utilized it as a catalyst to prepare various homopolymers and copolymers by sequential addition or redox switchable ROP. For example, we were able to obtain PLA homopolymers at 70 ^{o}C with good control, as evidenced by the agreement with the expected molar masses and narrow dispersity values. The ROP of other cyclic esters to obtain homopolymers such as PCL, PVL, PTMC, and PCHO was also carried out, however, with less control. In addition, several di-block copolymers, such as PTMC-PLA, PCL-PLA, and PTMC-PCHO, were prepared by sequential addition or one pot redox switchable ROP. The formation of copolymers was evidenced by changes in the corresponding GPC/SEC traces and ^{1}H NMR spectra.

We also studied the mechanism of Al catalyzed ROP both experimentally and theoretically. Detailed DFT studies revealed that the chelation of the carbonyl groups to the metal center plays an important role during the polymerization. For example, the insertion of the first LA is facile with both **1^{red}** and **1^{ox}**, however, after the first insertion of LA, the insertion of a second monomer (such as CL and TMC) is

much more difficult. On the other hand, in the reduced state, the insertion of CL or TMC will not lead to a significant change for the next insertion (propagation). However, in the oxidized state, the propagation step will be facilitated by the chelation effect, causing a faster propagation than initiation. The faster propagation than initiation usually translated into a less controlled polymerization, resulting in broad dispersity values and higher molar masses than expected. For example, the ROP of CL with the reduced state catalyst, $\mathbf{1^{red}}$, had similar activation barriers for the initiation and propagation steps. Based on these results, we propose that, with different ligands, the ROP of CL could vary from being uncontrolled to controlled.

For the ROP of LA, the propagation was usually much slower than initiation due to the chelation effect of the carbonyl group. We think that this effect is general, making the ROP of LA to be easily controlled with numerous catalysts. Understanding these results can help design novel catalyst systems. For example, a one-pot procedure for the selective copolymerization of LA and CL could be devised even though both monomers react with $\mathbf{1^{red}}$.

Moreover, based on the change in NBO charges from $\mathbf{1^{red}}$ to $\mathbf{1^{ox}}$, as well as the SOMO of $\mathbf{1^{ox}}$, we propose that the redox reactions occur on the ferrocene fragments. From the NBO studies, we also found out that the interactions between the Al center and the carbonyl groups are mainly dominated by electrostatic effects in the oxidized compounds. We anticipate that these findings could help us and others design novel catalysts to synthesize various multi-block copolymers efficiently in the future.

Experimental details

General considerations. All experiments were performed under a dry nitrogen atmosphere using standard Schlenk techniques or an MBraun inert-gas glove box. Solvents were purified using a two-column solid-state purification system by the method of Grubbs[111] and transferred to the glovebox without exposure to air. NMR solvents were obtained from Cambridge Isotope Laboratories, degassed, and stored over activated molecular sieves prior to use. ^{1}H and $^{19}F\{^{1}H\}$ NMR spectra were recorded on a Bruker300

spectrometer or a Bruker500 spectrometer at room temperature in C_6D_6. Chemical shifts are reported with respect to solvent residual peaks, 7.16 ppm (C_6D_6) and 7.26 ppm ($CDCl_3$). 2,4-di-*tert*-butylphenol, ^{n}BuLi, and boron trichloride were purchased from Sigma Aldrich and used as received. 1,3,5-Trimethoxybenzene was purchased from Sigma Aldrich and recrystallized from diethyl ether twice before use. $NaBAr^{F112}$ and $^{Ac}FcBAr^{F113}$ were synthesized following previously published procedures. H_2(thiolfan*) was synthesized by a modified method (see the Supporting Information for details) based on our previous report.[31] CH elemental analyses were performed on an Exeter Analytical, Inc. CE-440 Elemental Analyzer. Molar masses of the polymers were determined by GPC MALS. GPC MALS uses a Shimazu Prominence-i LC 2030C 3D equipped with an autosampler, two MZ Analysentechnik MZ-Gel SDplus LS 5 μm, 300 x 8mm linear columns, Wyatt DAWN HELEOS-II and Wyatt Optilab T-rEX. The column temperature was set at 40 °C. A flow rate of 0.70 mL/min was used and samples were dissolved in chloroform. dn/dc values for all homopolymers were calculated by making 4 to 6 solutions of increasing concentration (0.1 - 1.0 mg/mL), directly injecting them into the RI detector sequentially, and using the batch dn/dc measurement methods in the Astra software.

Cylic voltammetry. Cylic voltammetry studies were carried out in a 20 mL scintillation vial with electrodes fixed in position by a rubber stopper, in a 0.10 M $TBAPF_6$ (TBA = tetrabutylammonium) solution in tetrahydrofuran. A glassy carbon working electrode (planar circular area = 0.071 cm^2), a platinum reference electrode (planar circular area = 0.031 cm^2), and a silver-wire pseudo-reference electrode all purchased from CH Instruments. Before each cyclic voltammogram was recorded, the working and auxiliary electrodes were polished with an aqueous suspension of 0.05 μm alumina on a Microcloth polishing pad, after which the electrodes were rinsed with water and blotted dry with a Kimwipe. The electrodes were then brought into the glove box overnight under vacuum. Cyclic voltammograms were acquired with a CH Instruments CHI630D potentiostat and recorded with CH Instruments software (version 13.04) with data processing on Origin 9.1. All potentials are given with respect to the ferrocene-ferrocenium couple.

DFT calculations. All calculations were carried out with the GAUSSIAN 09 program package.[105] Geometry optimizations were performed with B3LYP.[114-116] The LANL2DZ basis set[117-119] with ECP was used for Fe, and the 6-31G(d) basis set[120-122] was used for other atoms. Frequency analysis was conducted at the same level of theory to verify that the stationary points are minima or saddle points. The single point energies and solvent effects in benzene were computed with PBE1PBE/[123]SDD-6-311+G(d,p) basis sets[124] by using the PCM solvation model.[125] The D3 version of Grimme's dispersion was applied for the dispersion correction.[107] All enthalpies and the Gibbs free energies are given in Hartree.

Synthesis of (thiolfan*)AlCl (1-Cl). To a toluene solution (3 mL) of H_2(salfan) (137.0 mg, 0.20 mmol), a toluene (2 mL) solution of $AlEt_2Cl$ (0.23 mL, 0.9 M in toluene, 0.21 mmol) was added dropwise at -78 °C, and the resulting mixture was stirred for 30 min. The reaction mixture was then brought to ambient temperature and stirred for 4 h. The volatiles were removed under reduced pressure and the residue was washed with cold hexanes. After washing, the solid was dried and yielded the pure product as a yellow powder. Yield: 122 mg, 85%. ^{1}H NMR (300 MHz, 25 ºC, C_6D_6), δ (ppm): 1.14 (s, 18H, ^{t}Bu), 1.82 (s, 18H, ^{t}Bu), 3.53 (br, 4H, Cp), 4.29 (br, 4H, Cp), 7.54 (d, 2H, *J* = 1.2 Hz, aromatic), 7.62 (d, 2H, *J* = 1.2 Hz, aromatic). ^{13}C NMR (75 MHz, 25 ºC, C_6D_6), δ (ppm): 29.8 (C(*C*H$_3$)$_3$), 31.6 (C(*C*H$_3$)$_3$), 34.5 (*C*(CH$_3$)$_3$), 36.1 (*C*(CH$_3$)$_3$), 71.0 (Cp), 120.9 (aromatic), 128.6 (aromatic), 129.3 (aromatic), 139.8 (aromatic), 141.9 (aromatic), 156.8 (aromatic).

Synthesis of (thiolfan*)Al(O^{t}Bu) (1^{red}). To a hexanes suspension (3 mL) of (thiolfan*)AlCl (122 mg, 0.17 mmol), a THF (3 mL) solution of KO^{t}Bu (21 mg, 0.19 mmol) was added at -78 °C, and the resulting mixture was stirred for 1 h. The reaction mixture was then brought to ambient temperature and stirred overnight. The volatiles were removed under reduced pressure, and the residue was re-dissolved in 3 mL toluene and passed through Celite to remove salts. The volatiles were removed under reduced pressure again to give **1^{red}** as a yellow powder. Yield: 124 mg, 96%. ^{1}H NMR (300 MHz, 25 ºC, C_6D_6), δ (ppm): 1.18 (s, 18H, ^{t}Bu), 1.35 (s, 9H, O^{t}Bu), 1.80 (s, 18H, ^{t}Bu), 3.62 (br, 4H, Cp), 4.27 (br, 4H, Cp), 7.54 (d,

2H, *J* = 1.2 Hz, aromatic), 7.60 (d, 2H, *J* = 1.2 Hz, aromatic). ^{13}C NMR (75 MHz, 25 ºC, C_6D_6), δ (ppm): 30.0 (C(*C*H$_3$)$_3$), 31.6 (C(*C*H$_3$)$_3$), 33.8 (OC(*C*H$_3$)$_3$), 34.4 (*C*(CH$_3$)$_3$), 36.0 (*C*(CH$_3$)$_3$), 69.4 (Cp), 70.5 (O*C*(CH$_3$)$_3$), 71.0 (Cp), 85.7 (Cp), 120.5 (aromatic), 127.1 (aromatic), 128.8 (aromatic), 139.3 (aromatic), 141.2 (aromatic), 157.3 (aromatic). Elemental analysis for $C_{42}H_{57}AlFeO_3S_2$ (756.86 g/mol): Calcd: 66.65% C, 7.59% H, 0.00% N; Found: 66.68% C, 7.67% H, 0.21% N.

Procedure for determining the reversibility of 1^{red} oxidation. To a C_6D_6 (0.6 mL) solution of (thiolfan*)Al(O^{t}Bu) (4 mg, 5 μmol) in a J-Young NMR tube, [^{Ac}Fc][BAr$^F_4$] (5 mg, 5 μmol) was added and the reaction was left at room temperature for 30 min. The reaction was monitored by ^{19}F NMR spectroscopy, showing a signal at -62.4 ppm that was assigned to **1^{ox}**. Then, an excess amount of $CoCp_2$ was added and the reaction was left at room temperature for another 1 h. The reaction was monitored by ^{19}F NMR spectroscopy again. No F peaks were observed at this point.

General procedure for the polymerization of one monomer by (thiolfan*)Al(O^{t}Bu). A solution of (thiolfan*)Al(O^{t}Bu) (1.9 mg, 2.5 μmol) in C_6D_6 (0.2 mL) was added to a solution of 1,3,5-trimethoxybenzene (8.4 mg, 50 μmol) and monomer (0.25 mmol) in C_6D_6 (0.4 mL). The solution was then transferred to a J-Young NMR tube, shaken, and moved to the corresponding reaction conditions.

General procedure for the polymerization of one monomer by [((thiolfan*)Al(O^{t}Bu)][BAr$^F_4$]. A solution of (thiolfan*)Al(O^{t}Bu) (1.9 mg, 2.5 μmol) in C_6D_6 (0.2 mL) was mixed with a slight excess of [^{Ac}Fc][BAr$^F_4$] (3.0 mg). The mixture was left for 15 min and then, it was added to a solution of 1,3,5-trimethoxybenzene (8.4 mg, 50 μmol) and monomer (0.25 mmol) in C_6D_6 (0.4 mL). The solution was then transferred to a J-Young NMR tube, shaken, and moved to the corresponding reaction conditions.

General procedure for the co-polymerization of monomer A and monomer B by (thiolfan*)Al(O^{t}Bu) or [(thiolfan*)Al(O^{t}Bu)][BAr$^F_4$] via sequential addition polymerization. (thiolfan*)Al(O^{t}Bu) (1.9 mg, 2.5 μmol) was dissolved in C_6D_6 (0.2 mL); if **1^{ox}** was used as the catalyst, [^{Ac}Fc][BAr$^F_4$] (3.0 mg) was added and the tube left for 15 min at ambient temperature. The solution of

the catalyst was added to a solution of monomer A (dissolved in 0.4 mL C_6D_6) in a J-Young NMR tube. The polymerization was run under the corresponding reaction conditions. After the first polymerization, the J-Young tube was cooled down to room temperature. Monomer B was dissolved in 0.2 mL of C_6D_6 and added to this J-Young tube. After the second polymerization, the reaction mixture was poured into cold methanol; a white solid precipitated that was filtered and dried.

General procedure for the co-polymerization of monomer A and monomer B by redox-switchable polymerization. (thiolfan*)Al(O^{t}Bu) (1.9 mg, 2.5 μmol) was dissolved in C_6D_6 (0.2 mL). The solution of the catalyst was added to the solution of monomer A (dissolved in 0.4 mL C_6D_6) in a J-Young NMR tube. The polymerization was run under the corresponding reaction conditions. After the first polymerization, the J-Young tube was cooled down to room temperature, [^{Ac}Fc][BAr$^F{}_4$] (3.0 mg) was then added and the tube left for 15 min. Monomer B was dissolved in 0.2 mL C_6D_6 and added to this J-Young tube. After the second polymerization, the reaction mixture was poured into cold methanol; a white solid precipitated that was filtered and dried.

ASSOCIATED CONTENT

Supporting Information

Experimental details, X-ray data and NMR spectra, and DFT calculation details. This material is available free of charge via the Internet at http://pubs.acs.org.

Corresponding Author

pld@chem.ucla.edu

Notes

The authors declare no competing financial interests.

ACKNOWLEDGMENT

The experimental work was supported by NSF, Grant 1362999 to PLD and CHE-1048804 for NMR spectroscopy, and the John Simon Guggenheim Memorial Foundation. The computational work used the Extreme Science and Engineering Discovery Environment (XSEDE), which is supported by the National Science Foundation grant ACI-1053575. MNR thanks the Clare Booth Luce Foundation for a scholarship.

REFERENCES

(1) Wu, J.; Yu, T.-L.; Chen, C.-T.; Lin, C.-C. Recent developments in main group metal complexes catalyzed/initiated polymerization of lactides and related cyclic esters. *Coord. Chem. Rev.* **2006**, *250*, 602-626.

(2) Ragauskas, A. J.; Williams, C. K.; Davison, B. H.; Britovsek, G.; Cairney, J.; Eckert, C. A.; Frederick, W. J.; Hallett, J. P.; Leak, D. J.; Liotta, C. L.; Mielenz, J. R.; Murphy, R.; Templer, R.; Tschaplinski, T. The Path Forward for Biofuels and Biomaterials. *Science* **2006**, *311*, 484-489.

(3) Gandini, A. Polymers from Renewable Resources: A Challenge for the Future of Macromolecular Materials. *Macromolecules* **2008**, *41*, 9491-9504.

(4) Childers, M. I.; Longo, J. M.; Van Zee, N. J.; LaPointe, A. M.; Coates, G. W. Stereoselective Epoxide Polymerization and Copolymerization. *Chem. Rev.* **2014**, *114*, 8129-8152.

(5) Drumright, R. E.; Gruber, P. R.; Henton, D. E. Polylactic Acid Technology. *Adv. Mater.* **2000**, *12*, 1841-1846.

(6) Dechy-Cabaret, O.; Martin-Vaca, B.; Bourissou, D. Controlled Ring-Opening Polymerization of Lactide and Glycolide. *Chem. Rev.* **2004**, *104*, 6147-6176.

(7) O'Keefe, B. J.; Hillmyer, M. A.; Tolman, W. B. Polymerization of lactide and related cyclic esters by discrete metal complexes. *J. Chem. Soc., Dalton Trans.* **2001**, 2215-2224.

(8) Kamber, N. E.; Jeong, W.; Waymouth, R. M.; Pratt, R. C.; Lohmeijer, B. G. G.; Hedrick, J. L. Organocatalytic Ring-Opening Polymerization. *Chem. Rev.* **2007**, *107*, 5813-5840.

(9) Brocas, A.-L.; Mantzaridis, C.; Tunc, D.; Carlotti, S. Polyether synthesis: From activated or metal-free anionic ring-opening polymerization of epoxides to functionalization. *Prog. Polym. Sci.* **2013**, *38*, 845-873.

(10) Keul, H.; Möller, M. Synthesis and degradation of biomedical materials based on linear and star shaped polyglycidols. *J. Polym. Sci. A Polym. Chem.* **2009**, *47*, 3209-3231.

(11) Coulembier, O.; Degée, P.; Hedrick, J. L.; Dubois, P. From controlled ring-opening polymerization to biodegradable aliphatic polyester: Especially poly(β-malic acid) derivatives. *Prog. Polym. Sci.* **2006**, *31*, 723-747.

(12) Dove, A. P. Controlled ring-opening polymerisation of cyclic esters: polymer blocks in self-assembled nanostructures. *Chem. Commun.* **2008**, 6446-6470.

(13) Labet, M.; Thielemans, W. Synthesis of polycaprolactone: a review. *Chem. Soc. Rev.* **2009**, *38*, 3484-3504.

(14) Place, E. S.; George, J. H.; Williams, C. K.; Stevens, M. M. Synthetic polymer scaffolds for tissue engineering. *Chem. Soc. Rev.* **2009**, *38*, 1139-1151.

(15) Williams, C. K.; Hillmyer, M. A. Polymers from Renewable Resources: A Perspective for a Special Issue of Polymer Reviews. *Polym. Rev.* **2008**, *48*, 1-10.

(16) Platel, R. H.; Hodgson, L. M.; Williams, C. K. Biocompatible Initiators for Lactide Polymerization. *Polym. Rev.* **2008**, *48*, 11-63.

(17) Williams, C. K. Synthesis of functionalized biodegradable polyesters. *Chem. Soc. Rev.* **2007**, *36*, 1573-1580.

(18) Dyer, H. E.; Huijser, S.; Susperregui, N.; Bonnet, F.; Schwarz, A. D.; Duchateau, R.; Maron, L.; Mountford, P. Ring-Opening Polymerization of rac-Lactide by Bis(phenolate)amine-Supported Samarium Borohydride Complexes: An Experimental and DFT Study. *Organometallics* **2010**, *29*, 3602-3621.

(19) Miranda, M. O.; DePorre, Y.; Vazquez-Lima, H.; Johnson, M. A.; Marell, D. J.; Cramer, C. J.; Tolman, W. B. Understanding the Mechanism of Polymerization of ε-Caprolactone Catalyzed by Aluminum Salen Complexes. *Inorg. Chem.* **2013**, *52*, 13692-13701.

(20) del Rosal, I.; Brignou, P.; Guillaume, S. M.; Carpentier, J.-F.; Maron, L. DFT investigations on the ring-opening polymerization of cyclic carbonates catalyzed by zinc-{[small beta]-diiminate} complexes. *Polym. Chem.* **2011**, *2*, 2564-2573.

(21) Guillaume, S. M.; Brignou, P.; Susperregui, N.; Maron, L.; Kuzdrowska, M.; Kratsch, J.; Roesky, P. W. Bis(phosphinimino)methanide borohydride complexes of the rare-earth elements as initiators for the ring-opening polymerization of trimethylene carbonate: combined experimental and computational investigations. *Polym. Chem.* **2012**, *3*, 429-435.

(22) von Schenck, H.; Ryner, M.; Albertsson, A.-C.; Svensson, M. Ring-Opening Polymerization of Lactones and Lactides with Sn(IV) and Al(III) Initiators. *Macromolecules* **2002**, *35*, 1556-1562.

(23) Chang, M.-C.; Lu, W.-Y.; Chang, H.-Y.; Lai, Y.-C.; Chiang, M. Y.; Chen, H.-Y.; Chen, H.-Y. Comparative Study of Aluminum Complexes Bearing N,O- and N,S-Schiff Base in Ring-Opening Polymerization of Îμ-Caprolactone and l-Lactide. *Inorg. Chem.* **2015**, *54*, 11292-11298.

(24) del Rosal, I.; Brignou, P.; Guillaume, S. M.; Carpentier, J.-F.; Maron, L. DFT investigations on the ring-opening polymerization of substituted cyclic carbonates catalyzed by zinc-{[small beta]-diketiminate} complexes. *Polym. Chem.* **2015**, *6*, 3336-3352.

(25) Marshall, E. L.; Gibson, V. C.; Rzepa, H. S. A Computational Analysis of the Ring-Opening Polymerization of rac-Lactide Initiated by Single-Site β-Diketiminate Metal Complexes: Defining the Mechanistic Pathway and the Origin of Stereocontrol. *J. Am. Chem. Soc.* **2005**, *127*, 6048-6051.

(26) Wang, L.; Kefalidis, C. E.; Sinbandhit, S.; Dorcet, V.; Carpentier, J.-F.; Maron, L.; Sarazin, Y. Heteroleptic Tin(II) Initiators for the Ring-Opening (Co)Polymerization of Lactide and Trimethylene Carbonate: Mechanistic Insights from Experiments and Computations. *Chem. Eur. J.* **2013**, *19*, 13463-13478.

(27) Tabthong, S.; Nanok, T.; Sumrit, P.; Kongsaeree, P.; Prabpai, S.; Chuawong, P.; Hormnirun, P. Bis(pyrrolidene) Schiff Base Aluminum Complexes as Isoselective-Biased Initiators for the Controlled Ring-Opening Polymerization of rac-Lactide: Experimental and Theoretical Studies. *Macromolecules* **2015**, *48*, 6846-6861.

(28) Broderick, E. M.; Guo, N.; Vogel, C. S.; Xu, C.; Sutter, J.; Miller, J. T.; Meyer, K.; Mehrkhodavandi, P.; Diaconescu, P. L. Redox Control of a Ring-Opening Polymerization Catalyst. *J. Am. Chem. Soc.* **2011**, *133*, 9278–9281.

(29) Quan, S. M.; Wang, X.; Zhang, R.; Diaconescu, P. L. Redox Switchable Copolymerization of Cyclic Esters and Epoxides by a Zirconium Complex. *Macromolecules* **2016**, *49*, 6768-6778.

(30) Romain, C.; Williams, C. K. Chemoselective Polymerization Control: From Mixed-Monomer Feedstock to Copolymers. *Angew. Chem. Int. Ed.* **2014**, *53*, 1607-1610.

(31) Wang, X.; Thevenon, A.; Brosmer, J. L.; Yu, I.; Khan, S. I.; Mehrkhodavandi, P.; Diaconescu, P. L. Redox Control of Group 4 Metal Ring-Opening Polymerization Activity toward l-Lactide and ε-Caprolactone. *J. Am. Chem. Soc.* **2014**, *136*, 11264-11267.

(32) Guillaume, S. M.; Kirillov, E.; Sarazin, Y.; Carpentier, J.-F. Beyond Stereoselectivity, Switchable Catalysis: Some of the Last Frontier Challenges in Ring-Opening Polymerization of Cyclic Esters. *Chem. Eur. J.* **2015**, *21*, 7988-8003.

(33) Blanco, V.; Leigh, D. A.; Marcos, V. Artificial switchable catalysts. *Chem. Soc. Rev.* **2015**, *44*, 5341-5370.

(34) Thevenon, A.; Garden, J. A.; White, A. J. P.; Williams, C. K. Dinuclear Zinc Salen Catalysts for the Ring Opening Copolymerization of Epoxides and Carbon Dioxide or Anhydrides. *Inorg. Chem.* **2015**, *54*, 11906-11915.

(35) Zhu, Y.; Romain, C.; Williams, C. K. Selective Polymerization Catalysis: Controlling the Metal Chain End Group to Prepare Block Copolyesters. *J. Am. Chem. Soc.* **2015**, *137*, 12179-12182.

(36) Paul, S.; Romain, C.; Shaw, J.; Williams, C. K. Sequence Selective Polymerization Catalysis: A New Route to ABA Block Copoly(ester-b-carbonate-b-ester). *Macromolecules* **2015**, *48*, 6047-6056.

(37) Biernesser, A. B.; Li, B.; Byers, J. A. Redox-Controlled Polymerization of Lactide Catalyzed by Bis(imino)pyridine Iron Bis(alkoxide) Complexes. *J. Am. Chem. Soc.* **2013**, *135*, 16553-16560.

(38) Brown, L. A.; Rhinehart, J. L.; Long, B. K. Effects of Ferrocenyl Proximity and Monomer Presence during Oxidation for the Redox-Switchable Polymerization of l-Lactide. *ACS Catal.* **2015**, *5*, 6057-6060.

(39) Gregson, C. K. A.; Gibson, V. C.; Long, N. J.; Marshall, E. L.; Oxford, P. J.; White, A. J. P. Redox Control within Single-Site Polymerization Catalysts. *J. Am. Chem. Soc.* **2006**, *128*, 7410-7411.

(40) Sauer, A.; Buffet, J.-C.; Spaniol, T. P.; Nagae, H.; Mashima, K.; Okuda, J. Switching the Lactide Polymerization Activity of a Cerium Complex by Redox Reactions. *ChemCatChem* **2013**, *5*, 1088-1091.

(41) Leibfarth, F. A.; Mattson, K. M.; Fors, B. P.; Collins, H. A.; Hawker, C. J. External Regulation of Controlled Polymerizations. *Angew. Chem. Int. Ed.* **2013**, *52*, 199-210.

(42) Quan, S. M.; Diaconescu, P. L. High activity of an indium alkoxide complex toward ring opening polymerization of cyclic esters. *Chem. Commun.* **2015**, *51*, 9643 - 9646.

(43) Broderick, E. M.; Guo, N.; Wu, T.; Vogel, C. S.; Xu, C.; Sutter, J.; Miller, J. T.; Meyer, K.; Cantat, T.; Diaconescu, P. L. Redox control of a polymerization catalyst by changing the oxidation state of the metal center. *Chem. Commun.* **2011**, *47*, 9897-9899.

(44) Abubekerov, M.; Shepard, S. M.; Diaconescu, P. L. Switchable Polymerization of Norbornene Derivatives by a Ferrocene-Palladium(II) Heteroscorpionate Complex. *Eur. J. Inorg. Chem.* **2016**, *2016*, 2634-2640.

(45) Abubekerov, M.; Diaconescu, P. L. Synthesis and Characterization of Ferrocene-Chelating Heteroscorpionate Complexes of Nickel(II) and Zinc(II). *Inorg. Chem.* **2015**, *54*, 1778–1784.

(46) Wang, X.; Brosmer, J. L.; Thevenon, A.; Diaconescu, P. L. Highly Active Yttrium Catalysts for the Ring-Opening Polymerization of ε-Caprolactone and δ-Valerolactone. *Organometallics* **2015**, *34*, 4700–4706.

(47) Brosmer, J. L.; Diaconescu, P. L. Yttrium-Alkyl Complexes Supported by a Ferrocene-Based Phosphinimine Ligand. *Organometallics* **2015**, *34*, 2567–2572.

(48) Upton, B. M.; Gipson, R. M.; Duhovic, S.; Lydon, B. R.; Matsumoto, N. M.; Maynard, H. D.; Diaconescu, P. L. Synthesis of ferrocene-functionalized monomers for biodegradable polymer formation. *Inorg. Chem. Front.* **2014**, *1*, 271 - 277.

(49) Shepard, S. M.; Diaconescu, P. L. Redox-Switchable Hydroelementation of a Cobalt Complex Supported by a Ferrocene-Based Ligand. *Organometallics* **2016**, *35*, 2446–2453.

(50) Huang, W.; Diaconescu, P. L. Reactivity and Properties of Metal Complexes Enabled by Flexible and Redox-Active Ligands with a Ferrocene Backbone. *Inorg. Chem.* **2016**, DOI: 10.1021/acs.inorgchem.1026b01118.

(51) Teator, A. J.; Lastovickova, D. N.; Bielawski, C. W. Switchable Polymerization Catalysts. *Chem. Rev.* **2016**, *116*, 1969-1992.

(52) Spassky, N.; Wisniewski, M.; Pluta, C.; Le Borgne, A. Highly stereoelective polymerization of rac-(D,L)-lactide with a chiral schiff's base/aluminium alkoxide initiator. *Macromol. Chem. Phys.* **1996**, *197*, 2627-2637.

(53) Dagorne, S.; Fliedel, C.: Organoaluminum Species in Homogeneous Polymerization Catalysis. In *Modern Organoaluminum Reagents: Preparation, Structure, Reactivity and Use*; Woodward, S., Dagorne, S., Eds.; Springer Berlin Heidelberg: Berlin, Heidelberg, 2012; pp 125-171.

(54) Ajellal, N.; Carpentier, J.-F.; Guillaume, C.; Guillaume, S. M.; Helou, M.; Poirier, V.; Sarazin, Y.; Trifonov, A. Metal-catalyzed immortal ring-opening polymerization of lactones, lactides and cyclic carbonates. *Dalton Trans.* **2010**, *39*, 8363-8376.

(55) Hormnirun, P.; Marshall, E. L.; Gibson, V. C.; White, A. J. P.; Williams, D. J. Remarkable Stereocontrol in the Polymerization of Racemic Lactide Using Aluminum Initiators Supported by Tetradentate Aminophenoxide Ligands. *J. Am. Chem. Soc.* **2004**, *126*, 2688-2689.

(56) Nomura, N.; Ishii, R.; Yamamoto, Y.; Kondo, T. Stereoselective Ring-Opening Polymerization of a Racemic Lactide by Using Achiral Salen– and Homosalen–Aluminum Complexes. *Chem. Eur. J.* **2007**, *13*, 4433-4451.

(57) Alcazar-Roman, L. M.; O'Keefe, B. J.; Hillmyer, M. A.; Tolman, W. B. Electronic influence of ligand substituents on the rate of polymerization of ε-caprolactone by single-site aluminium alkoxide catalysts. *Dalton Trans.* **2003**, 3082-3087.

(58) Nandi, P.; Matvieiev, Y. I.; Boyko, V. I.; Durkin, K. A.; Kalchenko, V. I.; Katz, A. MPV reduction using Al^{III}-calix[4]arene Lewis acid catalysts: Molecular-level insight into effect of ketone binding. *J. Cat.* **2011**, *284*, 42-49.

(59) Nandi, P.; Tang, W.; Okrut, A.; Kong, X.; Hwang, S.-J.; Neurock, M.; Katz, A. Catalytic consequences of open and closed grafted Al(III)-calix[4]arene complexes for hydride and oxo transfer reactions. *Proc. Natl. Acad. Sci. U.S.A.* **2013**, *110*, 2484-2489.

(60) Hohberger, C.; Spaniol, T. P.; Okuda, J. Living Polymerization by Bis(phenolate) Zirconium Catalysts: Synthesis of Isotactic Polystyrene-block-Polybutadiene Copolymers. *Macromol. Chem. Phys.* **2014**, *215*, 2001-2006.

(61) Tschage, M.; Jung, S.; Spaniol, T. P.; Okuda, J. Polymerization of Norbornene Using Chiral Bis(phenolate) Zirconium Catalysts. *Macromol. Rapid Commun.* **2015**, *36*, 219-223.

(62) Kapelski, A.; Okuda, J. Ring-opening polymerization of rac- and meso-lactide initiated by indium bis(phenolate) isopropoxy complexes. *J. Polym. Sci., Part A: Polym. Chem.* **2013**, *51*, 4983-4991.

(63) Sauer, A.; Buffet, J.-C.; Spaniol, T. P.; Nagae, H.; Mashima, K.; Okuda, J. Synthesis, Characterization, and Lactide Polymerization Activity of Group 4 Metal Complexes Containing Two Bis(phenolate) Ligands. *Inorg. Chem.* **2012**, *51*, 5764-5770.

(64) Peckermann, I.; Kapelski, A.; Spaniol, T. P.; Okuda, J. Indium Complexes Supported by 1,ϖ-Dithiaalkanediyl-Bridged Bis(phenolato) Ligands: Synthesis, Structure, and Controlled Ring-Opening Polymerization of l-Lactide. *Inorg. Chem.* **2009**, *48*, 5526-5534.

(65) Lian, B.; Ma, H.; Spaniol, T. P.; Okuda, J. Neutral and cationic aluminium complexes containing a chiral (OSSO)-type bis(phenolato) ligand: synthesis, structures and polymerization activity. *Dalton Trans.* **2009**, 9033-9042.

(66) Ma, H.; Spaniol, T. P.; Okuda, J. Rare-Earth Metal Complexes Supported by 1,ϖ-Dithiaalkanediyl-Bridged Bis(phenolato) Ligands: Synthesis, Structure, and Heteroselective Ring-Opening Polymerization of *rac*-Lactide. *Inorg. Chem.* **2008**, *47*, 3328-3339.

(67) Nakata, N.; Toda, T.; Ishii, A. Recent advances in the chemistry of Group 4 metal complexes incorporating [OSSO]-type bis(phenolato) ligands as post-metallocene catalysts. *Polym. Chem.* **2011**, *2*, 1597-1610.

(68) Saito, Y.; Nakata, N.; Ishii, A. Highly Isospecific Polymerization of Silyl-Protected ω-Alkenols Using an [OSSO]-Type Bis(phenolato) Dichloro Zirconium(IV) Precatalyst. *Macromol. Rapid Commun.* **2016**, *37*, 969-974.

(69) Hermans, C.; Rong, W.; Spaniol, T. P.; Okuda, J. Lanthanum complexes containing a bis(phenolate) ligand with a ferrocene-1,1'-diyldithio backbone: synthesis, characterization, and ring-opening polymerization of rac-lactide. *Dalton Trans.* **2016**, *45*, 8127-8133.

(70) Si, G.; Zhang, L.; Han, B.; Zhang, H.; Li, X.; Liu, B. Chromium complexes containing a tetradentate [OSSO]-type bisphenolate ligand as a novel family of catalysts for the copolymerization of carbon dioxide and 4-vinylcyclohexene oxide. *RSC Adv.* **2016**, *6*, 22821-22826.

(71) Si, G.; Zhang, L.; Han, B.; Duan, Z.; Li, B.; Dong, J.; Li, X.; Liu, B. Novel chromium complexes with a [OSSO]-type bis(phenolato) dianionic ligand mediate the alternating ring-opening copolymerization of epoxides and phthalic anhydride. *Polym. Chem.* **2015**, *6*, 6372-6377.

(72) Toda, T.; Nakata, N.; Matsuo, T.; Ishii, A. Synthesis, Structure, and 1-Hexene Polymerization Catalytic Ability of Group 5 Metal Complexes Incorporating an [OSSO]-Type Ligand. *ACS Catal.* **2013**, *3*, 1764-1767.

(73) Yamamoto, K.; Shibata, Y.; Kashiwa, Y.; Kondo, A.; Tsurugi, H.; Mashima, K. C–H Metalation Reaction of Diarylamine and Carbazole by Alkylaluminum Complexes at the Heteroatom-Bridged Dimeric Aluminum Core. *Eur. J. Inorg. Chem.* **2013**, *2013*, 3821-3825.

(74) Paek, C.; Kang, S. O.; Ko, J.; Carroll, P. J. Synthesis and Characterization of New Trinuclear Aluminum and Gallium Complexes of Bis(thiosemicarbazones). Single-Crystal Structure of (MeAl){CH_2[C(Me)NNC(S)N(Me)]$_2$}($AlMe_2$)$_2$. *Organometallics* **1997**, *16*, 1503-1506.

(75) Meduri, A.; Cozzolino, M.; Milione, S.; Press, K.; Sergeeva, E.; Tedesco, C.; Mazzeo, M.; Lamberti, M. Yttrium and aluminium complexes bearing dithiodiolate ligands: synthesis and application in cyclic ester polymerization. *Dalton Trans.* **2015**, *44*, 17990-18000.

(76) Yu, R.-C.; Hung, C.-H.; Huang, J.-H.; Lee, H.-Y.; Chen, J.-T. Four- and Five-Coordinate Aluminum Ketiminate Complexes: Synthesis, Characterization, and Ring-Opening Polymerization. *Inorg. Chem.* **2002**, *41*, 6450-6455.

(77) Lewiński, J.; Horeglad, P.; Tratkiewicz, E.; Grzenda, W.; Lipkowski, J.; Kolodziejczyk, E. Towards the Nature of Active Sites in Polymerization of Cyclic Esters Initiated by Aluminium Alkoxides: First Structurally Authenticated Aluminium-ε-Caprolactone Complex. *Macromol. Rapid Commun.* **2004**, *25*, 1939-1942.

(78) Biernesser, A. B.; Delle Chiaie, K. R.; Curley, J. B.; Byers, J. A. Block Copolymerization of Lactide and an Epoxide Facilitated by a Redox Switchable Iron-Based Catalyst. *Angew. Chem. Int. Ed.* **2016**, *55*, 5251–5254.

(79) Lewiński, J.; Horeglad, P.; Wójcik, K.; Justyniak, I. Chelation Effect in Polymerization of Cyclic Esters by Metal Alkoxides: Structure Characterization of the Intermediate Formed by Primary Insertion of Lactide into the Alâˆ’OR Bond of an Organometallic Initiator. *Organometallics* **2005**, *24*, 4588-4593.

(80) Gong, S.; Ma, H. β-Diketiminate aluminium complexes: synthesis, characterization and ring-opening polymerization of cyclic esters. *Dalton Trans.* **2008**, 3345-3357.

(81) Lv, K.; Cui, D. CCC-Pincer Bis(carbene) Lanthanide Dibromides. Catalysis on Highly cis-1,4-Selective Polymerization of Isoprene and Active Species. *Organometallics*, *29*, 2987-2993.

(82) Qian, F.; Liu, K.; Ma, H. Amidinate aluminium complexes: synthesis, characterization and ring-opening polymerization of rac-lactide. *Dalton Trans.* **2010**, *39*, 8071-8083.

(83) Yang, J.; Yu, Y.; Li, Q.; Li, Y.; Cao, A. Chemical synthesis of biodegradable aliphatic polyesters and polycarbonates catalyzed by novel versatile aluminum metal complexes bearing salen ligands. *J. Polym. Sci. A Polym. Chem.* **2005**, *43*, 373-384.

(84) Darensbourg, D. J.; Ganguly, P.; Billodeaux, D. Ring-Opening Polymerization of Trimethylene Carbonate Using Aluminum(III) and Tin(IV) Salen Chloride Catalysts. *Macromolecules* **2005**, *38*, 5406-5410.

(85) Hild, F.; Brelot, L.; Dagorne, S. Novel N,O,N-Supported Tetracoordinate Aluminum Complexes for the Highly Controlled and Immortal ROP of Trimethylene Carbonate (TMC) under Mild Conditions: Access to Narrowly Disperse poly-TMC and Derived Copolymers. *Organometallics* **2011**, *30*, 5457-5462.

(86) Ziegler, T. Approximate density functional theory as a practical tool in molecular energetics and dynamics. *Chem. Rev.* **1991**, *91*, 651-667.

(87) Ray, K.; Petrenko, T.; Wieghardt, K.; Neese, F. Joint spectroscopic and theoretical investigations of transition metal complexes involving non-innocent ligands. *Dalton Trans.* **2007**, 1552-1566.

(88) Frank, N. Prediction of molecular properties and molecular spectroscopy with density functional theory: From fundamental theory to exchange-coupling. *Coord. Chem. Rev.* **2009**, *253*, 526-563.

(89) Cramer, C. J.; Truhlar, D. G. Density functional theory for transition metals and transition metal chemistry. *Phys. Chem. Chem. Phys.* **2009**, *11*, 10757-10816.

(90) Alessandro, B. Some considerations on the proper use of computational tools in transition metal chemistry. *Inorg. Chim. Acta* **2008**, *361*, 3820-3831.

(91) Sousa, S. F.; Fernandes, P. A.; Ramos, M. J. General Performance of Density Functionals. *J. Phys. Chem. A* **2007**, *111*, 10439-10452.

(92) Park, Y.; Heo, J.; Baik, M.-H.; Chang, S. Why is the Ir(III)-Mediated Amido Transfer Much Faster Than the Rh(III)-Mediated Reaction? A Combined Experimental and Computational Study. *J. Am. Chem. Soc.* **2016**.

(93) Smith, K. T.; Berritt, S.; GonzÃ¡lez-Moreiras, M.; Ahn, S.; Smith, M. R.; Baik, M.-H.; Mindiola, D. J. Catalytic borylation of methane. *Science* **2016**, *351*, 1424-1427.

(94) Mazumder, S.; Crandell, D. W.; Lord, R. L.; Baik, M.-H. Switching the Enantioselectivity in Catalytic [4 + 1] Cycloadditions by Changing the Metal Center: Principles of Inverting the Stereochemical Preference of an Asymmetric Catalysis Revealed by DFT Calculations. *J. Am. Chem. Soc.* **2014**, *136*, 9414-9423.

(95) Fey, N. Lost in chemical space? Maps to support organometallic catalysis. *Chem. Cent. J.* **2015**, *9*, 1-10.

(96) Drew, K. L. M.; Baiman, H.; Khwaounjoo, P.; Yu, B.; Reynisson, J. Size estimation of chemical space: how big is it? *J. Pharm. Pharmacol.* **2012**, *64*, 490–495.

(97) Kirkpatrick, P.; Ellis, C. Chemical space. *Nature* **2004**, *432*, 823.

(98) Jover, J.; Fey, N. The computational road to better catalysts. *Chem. Asian J.* **2014**, *9*, 1714–1723.

(99) Foscato, M.; Venkatraman, V.; Occhipinti, G.; Alsberg, B. K.; Jensen, V. R. Automated building of organometallic complexes from 3D fragments. *J. Chem. Inf. Model.* **2014**, *54*, 1919–1931.

(100) Maldonado, A. G.; Hageman, J. A.; Mastroianni, S.; Rothenberg, G. Backbone diversity analysis in catalyst design. *Adv. Synth. Catal.* **2009**, *351*, 387–396.

(101) Fey, N.; Orpen, A. G.; Harvey, J. N. Building ligand knowledge bases for organometallic chemistry: computational description of phosphorus(III)-donor ligands and the metal-phosphorus bond. *Coord. Chem. Rev.* **2009**, *253*, 704–722.

(102) Fey, N. The contribution of computational studies to organometallic catalysis: descriptors, mechanisms and models. *Dalton Trans.* **2010**, *39*, 296–310.

(103) Burello, E.; Farrusseng, D.; Rothenberg, G. Combinatorial explosion in homogeneous catalysis: screening 60,000 cross-coupling reactions. *Adv. Synth. Catal.* **2004**, *346*, 1844–1853.

(104) Lameijer, E. W.; Kok, J. N.; Bäck, T.; Ijzerman, A. P. Mining a chemical database for fragment co-occurrence: discovery of "Chemical clichés". *J. Chem. Inf. Model.* **2006**, *46*, 553–562.

(105) Frisch, M. J.: Gaussian 09 (Revision D.01). Gaussian Inc.: Wallingford, CT, 2010 (see the SI for the full reference).

(106) Towns, J.; Cockerill, T.; Dahan, M.; Foster, I.; Gaither, K.; Grimshaw, A.; Hazlewood, V.; Lathrop, S.; Lifka, D.; Peterson, G. D.; Roskies, R.; Scott, J. R.; Wilkens-Diehr, N. XSEDE: Accelerating Scientific Discovery. *Computing in Science and Engineering*2014, p. 62.

(107) Grimme, S.; Antony, J.; Ehrlich, S.; Krieg, H. A consistent and accurate ab initio parametrization of density functional dispersion correction (DFT-D) for the 94 elements H-Pu. *J. Chem. Phys.* **2010**, *132*, 154104.

(108) Vanhoorne, P.; Dubois, P.; Jerome, R.; Teyssie, P. Macromolecular engineering of polylactones and polylactides. 7. Structural analysis of copolyesters of ε-caprolactone and L- or D,L-lactide initiated by triisopropoxyaluminum. *Macromolecules* **1992**, *25*, 37-44.

(109) Vion, J. M.; Jerome, R.; Teyssie, P.; Aubin, M.; Prudhomme, R. E. Synthesis, characterization, and miscibility of caprolactone random copolymers. *Macromolecules* **1986**, *19*, 1828-1838.

(110) Florczak, M.; Duda, A. Effect of the Configuration of the Active Center on Comonomer Reactivities: The Case of ε-Caprolactone/ l,l-Lactide Copolymerization. *Angew. Chem. Int. Ed.* **2008**, *47*, 9088-9091.

(111) Pangborn, A. B.; Giardello, M. A.; Grubbs, R. H.; Rosen, R. K.; Timmers, F. J. Safe and Convenient Procedure for Solvent Purification. *Organometallics* **1996**, *15*, 1518-1520.

(112) Reger, D.: Sodium Tetrakis(3,5-bis(trifluoromethyl)phenyl)borate, Na[B(3,5-$(CF_3)_2C_6H_3)_4$]. In *Inorganic Syntheses*; Shapley, J. R., Ed.; Wiley-Interscience, 2004; Vol. 34; pp 5.

(113) Dhar, D.; Yee, G. M.; Spaeth, A. D.; Boyce, D. W.; Zhang, H.; Dereli, B.; Cramer, C. J.; Tolman, W. B. Perturbing the Copper(III)–Hydroxide Unit through Ligand Structural Variation. *J. Am. Chem. Soc.* **2016**, *138*, 356-368.

(114) Becke, A. D. Density-functional thermochemistry. III. The role of exact exchange. *J. Chem. Phys.* **1993**, *98*, 5648-5652.

(115) Lee, C.; Yang, W.; Parr, R. G. Development of the Colle-Salvetti correlation-energy formula into a functional of the electron density. *Phys. Rev. B* **1988**, *37*, 785.

(116) Becke, A. D. A new mixing of Hartree – Fock and local density - functional theories. *J. Chem. Phys.* **1993**, *98*, 1372-1377.

(117) Hay, P. J.; Wadt, W. R. Ab initio effective core potentials for molecular calculations. Potentials for K to Au including the outermost core orbitals. *J. Chem. Phys.* **1985**, *82*, 299-310.

(118) Roy, L. E.; Hay, P. J.; Martin, R. L. Revised Basis Sets for the LANL Effective Core Potentials. *J. Chem. Theory Comput.* **2008**, *4*, 1029-1031.

(119) Ehlers, A. W.; Böhme, M.; Dapprich, S.; Gobbi, A.; Höllwarth, A.; Jonas, V.; Köhler, K. F.; Stegmann, R.; Veldkamp, A.; Frenking, G. A set of f-polarization functions for pseudo-potential basis sets of the transition metals Sc Cu, Y Ag and La Au. *Chem. Phys. Lett.* **1993**, *208*, 111-114.

(120) Ditchfield, R.; Hehre, W. J.; Pople, J. A. Self-Consistent Molecular-Orbital Methods. IX. An Extended Gaussian-Type Basis for Molecular-Orbital Studies of Organic Molecules. *J. Chem. Phys.* **1971**, *54*, 724-728.

(121) Hehre, W. J.; Ditchfield, R.; Pople, J. A. Self-Consistent Molecular Orbital Methods. XII. Further Extensions of Gaussian—Type Basis Sets for Use in Molecular Orbital Studies of Organic Molecules. *J. Chem. Phys.* **1972**, *56*, 2257-2261.

(122) Hariharan, P. C.; Pople, J. A. The influence of polarization functions on molecular orbital hydrogenation energies. *Theor. Chim. Acta* **1973**, *28*, 213-222.

(123) Perdew, J. P.; Burke, K.; Ernzerhof, M. Generalized Gradient Approximation Made Simple. *Phys. Rev. Lett.* **1996**, *77*, 3865-3868.

(124) Dolg, M.; Wedig, U.; Stoll, H.; Preuss, H. Energy‐adjusted abinitio pseudopotentials for the first row transition elements. *J. Chem. Phys.* **1987**, *86*, 866-872.

(125) Scalmani, G.; Frisch, M. J. Continuous surface charge polarizable continuum models of solvation. I. General formalism. *J. Chem. Phys.* **2010**, *132*, 114110.

TOC

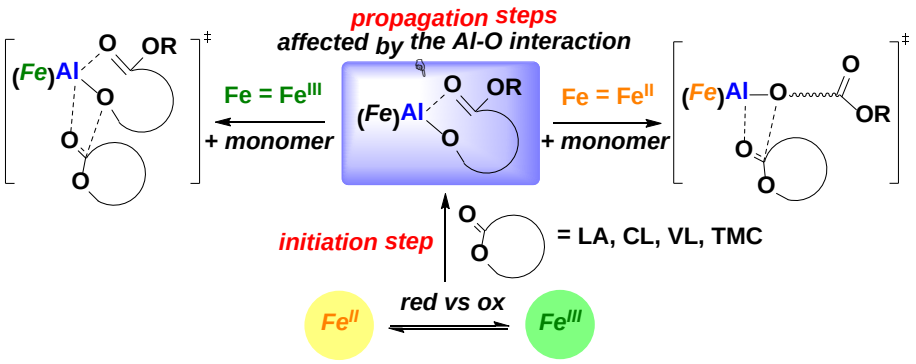
propagation steps
affected by the Al-O interaction
(Fe)Al
O
OR
Fe = Fe^III
+ monomer
Fe = Fe^II
+ monomer
initiation step
= LA, CL, VL, TMC
red vs ox
Fe^II
Fe^III